IFIC−01−0117
FTUV−01−0117

Meson exchange in the weak decay of Λ hypernuclei and the Γ_n/Γ_p ratio

D. Jido, E. Oset and J. E. Palomar

Departamento de Física Teórica e IFIC, Centro Mixto Universidad de Valencia-CSIC, 46100 Burjassot (Valencia), Spain

Abstract

We take an approach to the Λ non-mesonic weak decay in nuclei based on the exchange of mesons. The one pion and one kaon exchange are considered, together with the exchange of two pions, either correlated, leading to an important scalar-isoscalar exchange (σ-like exchange), or uncorrelated (box diagrams). Extra effects of omega exchange in the scalar-isoscalar channel are also considered. Constraints of chiral dynamics are used to generate these exchanges. A drastic reduction of the OPE results for the Γ_n/Γ_p ratio is obtained and the new results are compatible with all present experiments within errors. The absolute rates obtained for different nuclei are also in good agreement with experiment.

[Key Word] Λ weak decay, Γ_n/Γ_p ratio, chiral unitary theory.

1 Introduction

The problem of the Γ_n/Γ_p ratio is the most persistent and serious problem related to the non-mesonic decay of Λ hypernuclei. The problem lies in the large discrepancy between the theoretical ratio provided by the one pion exchange model (OPE) and the experiment. While certainly the OPE model is too simplified, the different attempts improving on the model for the non-mesonic decay have not been more successful. The OPE model, using exclusively the parity conserving part of the weak Λ decay vertex $H_{\Lambda\pi N}$, leads to a Γ_n/Γ_p ratio of 1/14 [1] in nuclear matter. The ratio is much influenced by the antisymmetry of the two-nucleon wave functions and if one neglects crossed terms this ratio becomes 1/5. If in addition one includes the parity violating term, which is less important than the parity conserving one for the non-mesonic decay, the ratio changes to about 1/8 [2]. These results are somewhat different in [3] where a ratio of about 1/5 is claimed for the ${}^{12}_{\Lambda}$C nucleus although a value of 1/11 is obtained in nuclear matter and the ${}^{5}_{\Lambda}$He nucleus. Results become worse when short range correlations are taken into account and the values range from 1/16 in [4], to 1/8 in [5], 1/14 in [2] and 1/20 in [3], all of them for ${}^{5}_{\Lambda}$He. The ratios are somewhat larger for ${}^{12}_{\Lambda}$C, 1/10 in [2] and 1/5 in [3].

There are still some discrepancies as to the precise numbers but there is a systematic agreement in the fact that they range from about 1/5 to 1/20 and that numbers of the order of unity, as experiments suggest, cannot be accommodated with the OPE model.

Experimentally one has results for ${}^{5}_{\Lambda}$He from [6] with a ratio 0.93±0.5 and for ${}^{12}_{\Lambda}$C with ratios $1.33^{+1.12}_{-0.81}$ [6], $1.87^{+0.91}_{-1.59}$ [7] and 0.70±0.30, 0.52±0.16 [8]. More recent results for ${}^{12}_{\Lambda}$C are still quoted as preliminary [9, 10] but also range in values around unity with large errors.

The large discrepancy of the OPE predictions with the experimental data has stimulated much theoretical work. One line of progress has been the extension of the one meson exchange model including the exchange of $\rho, \eta, K, \omega, K^*$ in [2] and [3]. The results obtained are somewhat contradictory since while in [3] values for the Γ_n/Γ_p ratio around 0.83 are quoted for ${}^{12}_{\Lambda}$C, the number quoted in [2] is 0.07. Also, in [2] the same ratio is obtained for ${}^{5}_{\Lambda}$He and ${}^{12}_{\Lambda}$C while in [3] the value of the ratio in ${}^{12}_{\Lambda}$C is about twice larger than for ${}^{5}_{\Lambda}$He (see [11] for a further discussion on this issue).

Another line of progress has been the consideration of two pion exchange. An early attempt in [12] including N and Σ intermediate states in a box diagram with two pions did not improve on the ratio and it made it actually slightly worse. However, in [13] the Δ intermediate states were also considered leading to an increase of the the Γ_n/Γ_p ratio, although no numbers were given. A similar approach was followed in [14, 15] where the exchange of two interacting pions through the σ resonance was considered and found to lead also to improved results in the Γ_n/Γ_p ratio. Although there are still some differences in the works and results of [14, 15] (see [11] for details) they share the qualitative conclusion that the Γ_n/Γ_p ratio increases when the σ exchange is considered. In [14] the ratio goes from 0.087 for only pion exchange to 0.14 when the correlated two pions in the σ channel (and also the ρ, which does not change much the ratio) are considered.

A third line followed so far has been to take the quark model point of view. The origins of this line of work come from the pioneering work of [16], where pion exchange was considered beyond a certain distance and quark degrees of freedom before. Two recent works follow this line [5, 17] although there are some discrepancies between them and some sign ambiguity that has been recently clarified using arguments of current algebra in [18]. Quoting the results from this latter work, the Γ_n/Γ_p ratio is changed from 0.13 for the OPE model to 0.49 when the quark degrees of freedom are considered in the nucleus of ${}^{5}_{\Lambda}$He. Further work is done in [19], where considerations of chiral symmetry are done and interesting new relations are developed, but the conclusion is that, though the consideration of the quark degrees of freedom at short distances goes in the direction of improving the Γ_n/Γ_p ratio, the large contribution of the OPE makes the final ratios still incompatible with experimental results. However, some recent advances in this direction, including K exchange, [20, 21] lead to improved ratios but also large widths.

Some hopes were raised when the mechanism of the two-nucleon induced Λ decay was introduced in [22] where the Λ decays into a nucleon and a virtual pion which is absorbed by two nucleons. The absorption of pions takes place mostly on neutron proton pairs, thus leading to a mechanism that produces two neutrons and a proton per Λ decay. This enhances the production of neutrons versus protons and could be responsible for the large number of neutrons seen in the experiment without the need to have a large value for the Γ_n/Γ_p ratio of the one-nucleon induced Λ decay. However, it was observed in [23] that this had to be taken with care and, given the type of experimental analysis done to extract the Γ_n/Γ_p ratio, the consideration of this new mode made the experimental ratio even bigger, depending on the number obtained from the analysis without considering the two-nucleon mode. Actually, as noted in [24], the results of the new analysis depend on whether the slow particles are

detected or not. A detailed analysis of this problem considering final state interaction of the nucleons and actual detection thresholds was done in [25] determining spectra of neutrons and protons from where future experiments can extract the Γ_n/Γ_p ratio. For the purpose of the present paper the findings of [25] simply tell us that the consideration of the two-nucleon mode of Λ decay makes the experimental errors a little larger than assumed so far from present analyses.

The situation is hence puzzling. Discrepancies between authors using a similar approach still persist, but in spite of that, there is a clear discrepancy between predictions of different models and present experimental results.

Our contribution to this problem has certainly benefitted from previous efforts and we have included in our approach in a unified way all the relevant elements considered before within the context of the one and two meson exchange. Thus, we include pion exchange, short range correlations via the Landau-Migdal interaction, which also serves to estimate the effects of the ρ meson or K^* exchange, kaon exchange, the exchange of two pions, uncorrelated or interacting in the scalar-isoscalar channel (the σ channel) and omega exchange. The correlated two pion exchange has been done here following closely the steps of the recent work [26] where the two pions are allowed to interact, using the Bethe-Salpeter equation and the chiral Lagrangians [27]. This chiral unitary approach to the $\pi\pi$ scattering problem leads to good agreement with the $\pi\pi$ data in the scalar sector including the generation of a pole in the t-matrix corresponding to the σ meson [28]. We also study the ω exchange which is of the same order of magnitude.

The results obtained here lead to ratios of Γ_n/Γ_p of the order of 0.53 and simultaneously one can obtain values for the absolute rates of different nuclei that are comparable to the experimental ones using reasonable Landau-Migdal parameters for the strong p-wave interactions. These high values obtained for Γ_n/Γ_p are compatible with all present experiments within errors, even more if these errors are enlarged as suggested in [25].

The present calculations are done in nuclear matter and the local density approximation is used to go to finite nuclei. The procedure should be quite good for nuclei around ${}^{12}_{\Lambda}$C and heavier, as done here. Yet, given the particular significance that the present findings have, apparently solving a long standing problem, additional calculations in finite nuclei should be encouraged and work in this direction is already under way [29].

The paper is organized as follows. In the next section we review the OPE approach. In section 3 the kaon exchange is introduced. The two-pion exchange is included in section 4 and the results are presented and discussed in section 5. Conclusions are then presented in the last section.

2 One Pion Exchange

The decay of the Λ in nuclear matter is investigated here with the propagator approach which provides a unified picture of different decay channels of the Λ [30]. As mentioned above, the decay width of the Λ is calculated in infinite nuclear matter, and is extended to finite nuclei with the local density approximation. In this section we shall review the calculation of the decay width of the Λ in nuclear matter using the one pion exchange approach.

First of all, we start with an effective $\pi\Lambda N$ weak interaction which is written as,

$$\mathcal{L}_{\Lambda N\pi} = -iG\mu^2\bar{\psi}_N[A+\gamma_5 B]\vec{\tau}\cdot\vec{\phi}_\pi\psi_\Lambda + \text{h.c.} \tag{1}$$

after the non-relativistic reduction we have:

$$\mathcal{L}_{\Lambda N\pi} = -iG\mu^2\bar{\psi}_N[S - (P/\mu)\vec{\sigma}\cdot\vec{q}]\vec{\tau}\cdot\vec{\phi}_\pi\psi_\Lambda + \text{h.c.} \tag{2}$$

where μ denotes the pion mass, and G is the weak coupling constant with

$$G\mu^2 = 2.211 \times 10^{-7} \tag{3}$$

and $\vec{q}$ is the momentum of the outgoing pion.

By assuming that the Λ behaves as a $I = 1/2, I_z = -1/2$ state in the isospin space, this effective interaction already implements the phenomenological $\Delta I = 1/2$ rule, which is seen in the nonleptonic free decay of the Λ. The coupling constants S and P are determined by the parity conserving and parity violating amplitudes of the nonleptonic Λ decay, respectively:

$$A = S = 1.06, \qquad \frac{B}{2M_N}\mu = -P = -0.527 \tag{4}$$

with M_N the nucleon mass. The πNN vertex with strong interaction is given by the following effective Lagrangian:

$$\mathcal{L}^S_{\pi NN} = -\frac{g}{2M_N}\bar{\psi}_N\gamma^\mu\gamma_5\vec{\tau}\cdot\partial_\mu\vec{\phi_\pi}\psi_N \tag{5}$$

or, after the non-relativistic reduction,

$$\mathcal{L}^S_{\pi NN} = -i\frac{f_{\pi NN}}{\mu}\bar{\psi}_N\vec{\sigma}\cdot\vec{q}\vec{\tau}\cdot\vec{\phi_\pi}\psi_N \tag{6}$$

with $f_{\pi NN} = g\mu/2M_N = 1.02$, and an incoming pion of momentum $\vec{q}$.

In order to evaluate the Λ decay width Γ in a nuclear medium due to a certain $\Lambda N \to NN$ transition amplitude, as depicted in fig. 1, we start with the calculation of the self-energy in the medium, Σ, shown in fig. 2, and then we take its imaginary part:

$$\Gamma = -2 \text{ Im } \Sigma \tag{7}$$

We take into account the ph and Δh excitations to all orders in the sense of the random phase approximation (RPA), which is shown in fig. 3. This induces modifications of the pion propagation. On the other hand, short range correlations modulate the $\Lambda N \to NN$ transition amplitude in coordinate space and induce changes in the momentum space representation (see Appendix). The p-wave (parity conserving) part of the weak $\Lambda N \to NN$ transition is then written as

$$G^{\pi,\text{p-wave}}_{\Lambda N\to NN}(q) = [V_l'(q)\hat{q}_i\hat{q}_j + V_t'(q)(\delta_{ij} - \hat{q}_i\hat{q}_j)]\sigma_i^{(1)}\sigma_j^{(2)}\vec{\tau}^{(1)}\cdot\vec{\tau}^{(2)} \tag{8}$$

with

$$V_l'(q) = \frac{f_{\pi NN}}{\mu}\frac{P}{\mu}[\vec{q}^{\,2}D_\pi(q)F_\pi^2(q) + g_l^\Lambda(q)] \tag{9}$$

$$V_t'(q) = \frac{f_{\pi NN}}{\mu}\frac{P}{\mu}g_t^\Lambda(q)\ , \tag{10}$$

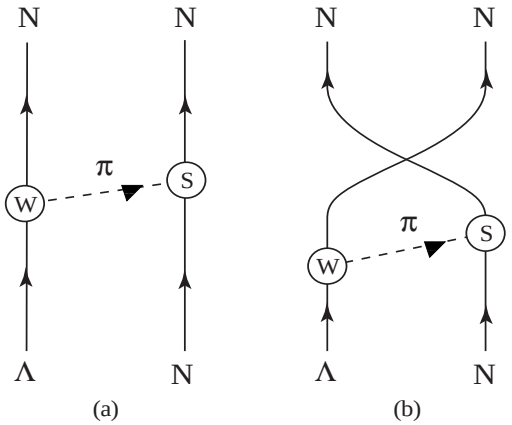

Figure 1: Non-mesonic decay of Λ with one π exchange. (a) and (b) denote the direct and exchange diagrams, respectively.

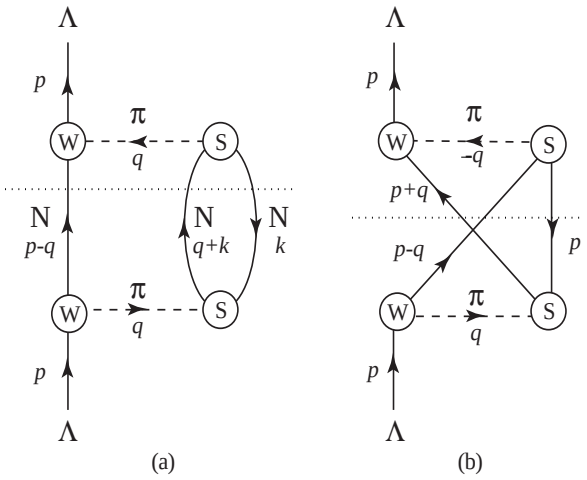

Figure 2: Lowest order self-energy of the Λ. The cut gives the width of the Λ for the corresponding non-mesonic decay of fig. 1.

while the s-wave parity violating part gives rise to

$$G^{\pi,\mathrm{s-wave}}_{\Lambda N\to NN}(q) = V'_s(q)\ \hat{q}_i\ \sigma_i^{(2)}\ \vec{\tau}^{(1)}\cdot\vec{\tau}^{(2)}\ , \tag{11}$$

with

$$V'_s(q) = \frac{f_{\pi NN}}{\mu} S[D_\pi(q)F_\pi^2(q) + g_s^\Lambda(q)]|\vec{q}| \tag{12}$$

Here $g_l^\Lambda(q)$, $g_t^\Lambda(q)$ and $g_s^\Lambda(q)$ implement the short range correlations, with a similar role to that of the Landau-Migdal parameters, and $D_\pi(q)$ and $F_\pi(q)$ denote the pion propagator and form factor, respectively. We use the same form factor $F_\pi(q)$ in both strong and weak vertices:

$$F_\pi(q) = \frac{\Lambda_\pi^2}{\Lambda_\pi^2 - q^2} \tag{13}$$

We have similar expressions for the spin-isospin strong effective interaction, which we write as

$$G_{NN}(q) = [V_l(q)\hat{q}_i\hat{q}_j + V_t(q)(\delta_{ij} - \hat{q}_i\hat{q}_j)]\sigma_i^{(1)}\sigma_j^{(2)}\vec{\tau}^{(1)}\cdot\vec{\tau}^{(2)} \tag{14}$$

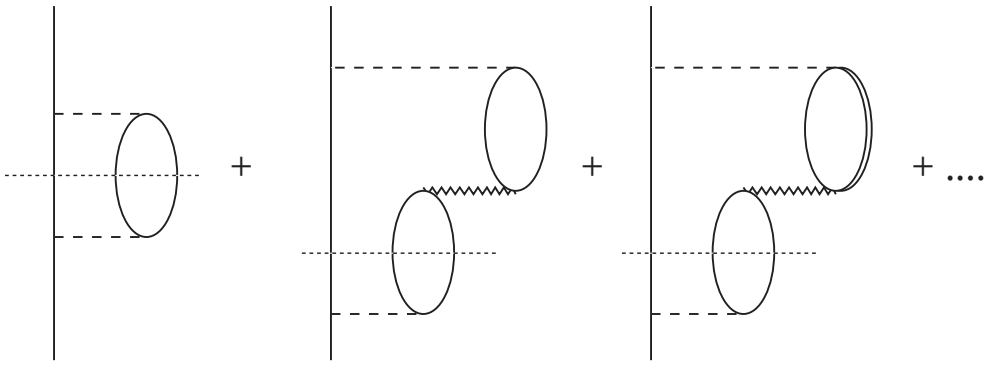

Figure 3: The medium corrections to the Λ self-energy shown in fig. 2.

with

$$V_l(q) = \frac{f_{\pi NN}^2}{\mu^2}[\vec{q}^{\,2} D_\pi(q) F_\pi^2(q) + g_l(q)] \tag{15}$$

$$V_t(q) = \frac{f_{\pi NN}^2}{\mu^2}[\vec{q}^{\,2} D_\rho(q) F_\rho^2(q) C_\rho + g_t(q)] \tag{16}$$

It is worth noting that the first ph and Δh excitations in fig. 3 are induced by the weak transition $G_{\Lambda N\to NN}(q)$, but, once it happens, the successive excitations are produced by the strong transition $G_{NN}(q)$ or the analogous one with $G_{N\Delta}(q)$.

The short range correlations, $g_l(q)$ and $g_t(q)$, which are written explicitly in eqs. (67, 68) in the Appendix, have slightly smaller size than those used in the conventional analysis of the spin-isospin effective nuclear force [31]. Thus we rescale these functions $g_l(q)$ and $g_t(q)$ so that they have the value $g' = 0.7$ at $q = 0$.

In the nucleon propagator, the Pauli blocking effect is implemented in terms of the nucleon occupation number $n(\vec{k})$:

$$G_N(k) = \frac{1 - n(\vec{k})}{k^0 - E(\vec{k}) - V_N + i\epsilon} + \frac{n(\vec{k})}{k^0 - E(\vec{k}) - V_N - i\epsilon} \tag{17}$$

where the nucleon binding energy $V_N = -k_F^2/2M_N$ from the Thomas-Fermi approximation and $n(\vec{k}) = 1$ for $|\vec{k}| \le k_F$, $n(\vec{k}) = 0$ for $|\vec{k}| > k_F$ with k_F the Fermi momentum, which depends on the position of the Λ through the density $\rho(r)$ in the local density approximation.

After the summation of the RPA series, the non-mesonic decay width coming from the direct term, shown in fig. 1(a), is obtained with the result [30]:

$$\Gamma(k,\rho) = -(G\mu^2)^2 \int \frac{d^3q}{(2\pi)^3}\theta(q_0)[1 - n(\vec{k} - \vec{q})]\,\mathrm{Im}\,W(q)|_{q^0 = k^0 - E(\vec{k}-\vec{q}) - V_N}$$

$$\mathrm{Im}\,W(q) = \mathrm{Im}\,U_N(q)\; T(q) \tag{18}$$

with:

$$T^\pi_{p,\mathrm{dir}}(q) = \left[5\frac{V_s'^2(q)}{|1 - UV_l(q)|^2} + 5\frac{V_l'^2(q)}{|1 - UV_l(q)|^2} + 10\frac{V_t'^2(q)}{|1 - UV_t(q)|^2}\right]$$

$$T^\pi_{n,\mathrm{dir}}(q) = \left[\frac{V_s'^2(q)}{|1 - UV_l(q)|^2} + \frac{V_l'^2(q)}{|1 - UV_l(q)|^2} + 2\frac{V_t'^2(q)}{|1 - UV_t(q)|^2}\right] \tag{19}$$

$T^{\pi}_{p,\mathrm{dir}}$ and $T^{\pi}_{n,\mathrm{dir}}$ together with eq. (18) give the Λ decay induced by proton and neutron, respectively. Here $U(q) = U_N(q) + U_\Delta(q)$, and U_N and U_Δ are the Lindhard functions for ph and Δh excitations. To obtain eqs. (19) we take the spin average of Λ which removes the term linear in $\vec{\sigma}$ in the Λ self-energy.

Up to here we have only considered the direct term. Actually the contribution from the exchange terms, shown in fig. 2(b) is suppressed by factor 1/2 compared with the direct term, due to the absence of the nucleon loop. Isospin indices will be taken into account explicitly. However, as we shall see later, the exchange term gives a large contribution to the ratio of the neutron induced decay to the proton induced one.

To calculate the exchange term shown as fig. 2(b), we may use the same set of propagator with the direct term. In fact, assuming the Λ at rest, the variable in the upper propagator in fig. 2(b) is $-\vec{q}-\vec{p}$ instead of $\vec{q}$ in the direct diagram. However since q is large ($\sim$ 420 MeV/c) and p (the momentum of the occupied nucleons in the Fermi sea) is smaller than q and sometimes adds and other subtracts to $\vec{q}$, the corrections are of order $(p/q)^2$, and hence $(p/q)^2$ is about 20% in a term with smaller strength than the direct term and we neglect p in this interaction in front of $\vec{q}$. Therefore the difference in the calculation of the contribution from the exchange terms is the summation of spin and isospin. For the spin summation, it is important to notice that the upper pion carries momentum $-q$, which produces a different sign in the parity violating part with respect to the direct term. We calculate the spin sum of the exchange term for the parity violating part:

$$\frac{1}{2}\sum_s \langle s|\sigma^j\sigma^l|s\rangle \hat{q}_j\hat{q}_l i(-iV_s')i(iV_s') = -V_s'^2 \tag{20}$$

This gives the same sign as the direct term when including in the latter the minus sign due to the fermion loop. The spin sum for the p-wave in the exchange term is given by:

$$\begin{aligned}
&\frac{1}{2}\sum_s \langle s|\sigma^i\sigma^k\sigma^j\sigma^l|s\rangle \\
&\qquad \times\{V_l'\hat{q}_i\hat{q}_j + V_t'(\delta_{ij}-\hat{q}_i\hat{q}_j)\}\{V_l'\hat{q}_k\hat{q}_l + V_t'(\delta_{kl}-\hat{q}_k\hat{q}_l)\} &(21)\\
&= \quad V_l'^2 - 4V_l'V_t' &(22)
\end{aligned}$$

Note that $V_t'^2$ vanishes but a crossed term between V_l' and V_t' remains.

In fig. 4 one can see the different OPE diagrams corresponding to the $\Lambda p \to np$ and $\Lambda n \to nn$ transitions. We finally obtain:

$$T^{\pi}_{p,\mathrm{exch}} = -\frac{2V_s'^2}{|1-UV_l|^2} + \frac{2V_l'^2}{|1-UV_l|^2} - 8V_l'V_t'\mathrm{Re}\left[\frac{1}{(1-UV_l)(1-U^*V_t)}\right] \tag{23}$$

$$T^{\pi}_{n,\mathrm{exch}} = \frac{\frac{1}{2}V_s'^2}{|1-UV_l|^2} - \frac{\frac{1}{2}V_l'^2}{|1-UV_l|^2} + 2V_l'V_t'\mathrm{Re}\left[\frac{1}{(1-UV_l)(1-U^*V_t)}\right] \tag{24}$$

With the direct and exchange terms we obtain the non-mesonic decay width with one pion exchange. As we shall discuss later, if we add the mesonic width and the two-nucleon induced width we obtain $\Gamma_{tot} = 1.6\ \Gamma_\Lambda^{free}$, which is larger than the experimental width. If we neglect the transverse part and the induced interaction and we take only the direct terms, the ratio Γ_n/Γ_p is 1/5. However with the exchange terms, it becomes

$$\frac{\Gamma_n}{\Gamma_p} = \frac{\frac{3}{2}\Gamma_S + \frac{1}{2}\Gamma_P}{3\Gamma_S + 7\Gamma_P} \tag{25}$$

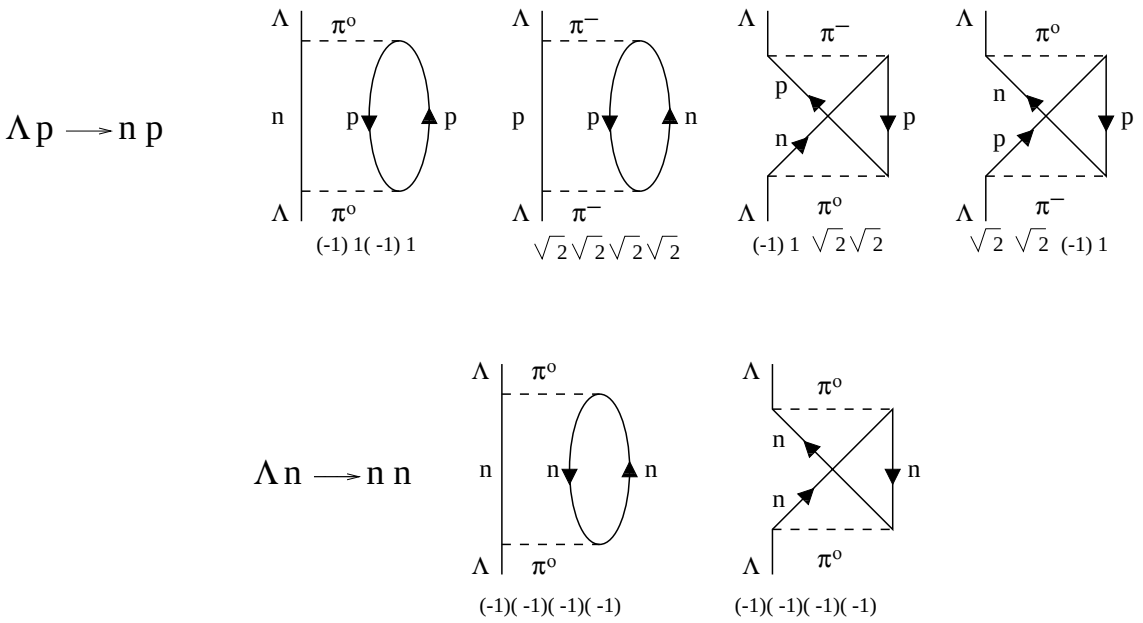

Figure 4: The isospin factors of the direct and exchange terms induced by proton and neutron. Recall that there is an extra relative minus sign for the exchange terms because of the absence of a fermion loop with respect to the direct term.

where Γ_S and Γ_P denote the partial width of the parity violating and parity conserving decay. Eq. (25) gives $\Gamma_n/\Gamma_p = 1/2 \sim 1/14$ (the values 1/2 and 1/14 are obtained when considering only s-wave and p-wave respectively). Therefore the exchange terms should be counted to reproduce both the total decay width and the Γ_n/Γ_p ratio. An actual calculation with all terms included gives $\Gamma \sim 1.1\ \Gamma_\Lambda^{free}$ and $\Gamma_n/\Gamma_p \sim 1/8$ for ${}^{12}_{\Lambda}$C. This implies that we need some extra mechanisms additional to that of pion exchange.

3 Kaon Exchange

The Λ non-mesonic decay with one K exchange takes place through the diagram shown in fig. 5. Including the K exchange is straightforward in the meson propagator approach, once the KNN weak vertex is fixed.

The strong $K\Lambda N$ vertex is given by:

$$\mathcal{L}^S_{K\Lambda N} = -\frac{g_{K\Lambda N}}{2M_N}\bar{\psi_N}\gamma^\mu\gamma_5\partial_\mu\phi_K\psi_\Lambda + \text{h.c.} \tag{26}$$

with $g_{K\Lambda N} \equiv f_{K\Lambda N} 2M/\mu$, which is estimated with the $SU(3)$ flavor symmetry:

$$\frac{f_{K\Lambda N}}{\mu} = -\frac{D+3F}{2\sqrt{3}f} \tag{27}$$

with $D+F = 1.26$, $D-F = 0.33$ and f the pion decay constant, $f = 93$ MeV. Note that there is a different sign in $f_{K\Lambda N}$ with respect to the $pp\pi^0$ vertex, $f_{\pi NN}/\mu = (D+F)/(2f)$.

The weak vertex of NNK may be written as

$$\mathcal{L}_{KNN} \;=\; -iG\mu^2\left[\bar{\psi}_p(A^{\bar{K}^0,p} + \gamma_5 B^{\bar{K}^0,p})\phi^\dagger_{K^0}\psi_p\right.$$

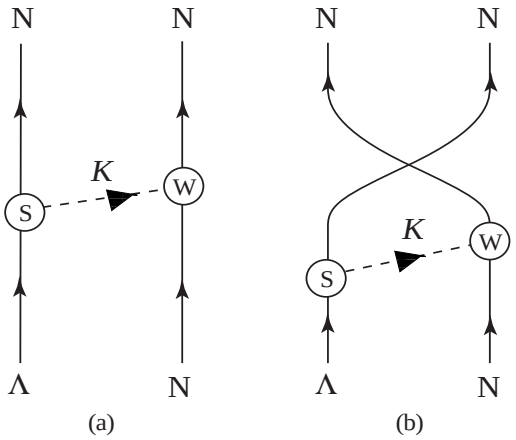

Figure 5: Non-mesonic decay of the Λ with one K exchange. (a) and (b) denote the direct and exchange diagrams, respectively.

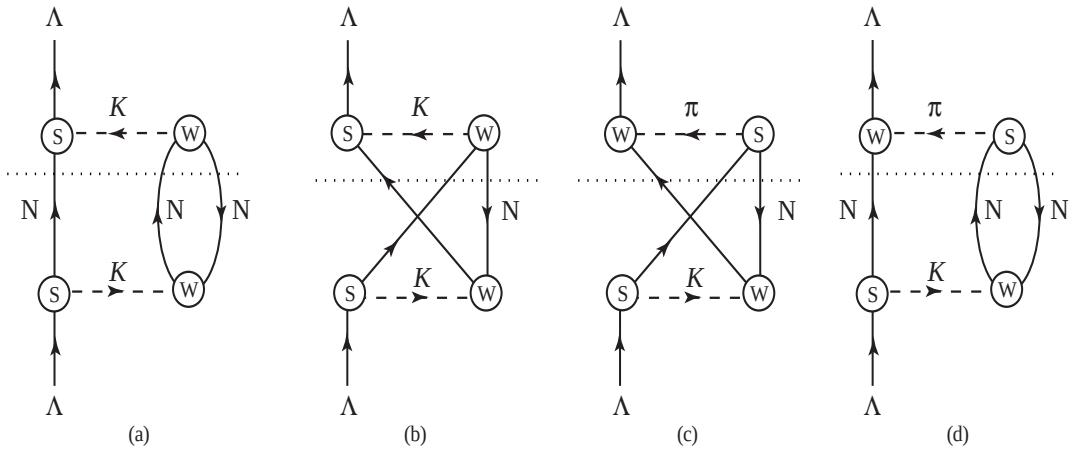

Figure 6: Lowest order self-energy of the Λ. The cut gives the width of the Λ for the corresponding non-mesonic decay to fig. 5(a) and (b). The diagrams (c) and (d) are the interference terms between π and K.

$$\begin{aligned} &+\bar{\psi}_n(A^{K^-,p}+\gamma_5 B^{K^-,p})\phi^\dagger_{K^+}\psi_p \\ &+\bar{\psi}_n(A^{\bar{K}^0,n}+\gamma_5 B^{\bar{K}^0,n})\phi^\dagger_{K^0}\psi_n\Big] \ + \text{h.c.} \end{aligned} \tag{28}$$

It is convenient to write these couplings in terms of S and P for the pion exchange, hence we introduce the factor $C^{K,N}$ as

$$A^{K,N} \equiv S^{K,N} = C_S^{K,N} S \qquad \frac{B^{K,N}}{2M_N}\mu \equiv C_P^{K,N} P \tag{29}$$

To avoid confusion recall that in the case of the pion there was a minus sign connecting B and P which we omit deliberately here to define the constants $C_P^{K,N}$. Isospin symmetry gives one constraint [3]:

$$C_S^{\bar{K}^0,n} = C_S^{\bar{K}^0,p} + C_S^{K^-,p} \qquad C_P^{\bar{K}^0,n} = C_P^{\bar{K}^0,p} + C_P^{K^-,p} \tag{30}$$

	PV	PC
π	$S = 1.05$	$P = 0.527$
K	$C_S^{\bar{K}^0 p} = 1.94$	$C_P^{\bar{K}^0 p} = 0.93$
	$C_S^{K^- p} = 0.76$	$C_P^{K^- p} = -2.64$
	$C_S^{\bar{K}^0 n} = 2.70$	$C_P^{\bar{K}^0 n} = -1.72$

Table 1: Coupling constants in the weak interaction.

The coupling constants $C^{K,N}$ should be determined by some theoretical analysis, because the KNN vertex cannot be determined directly by the experiment. Here we take the result of the conventional analysis of [3], where for the parity violating part the amplitude is assumed to behave as the 6^{th} component of the SU(3) generators, and for the parity conserving part the pole model is used. The values of $C^{K,N}$ are summarized in table 1.

Now we include one K exchange in the previous result. In the K exchange the positions of weak and strong vertex are opposite to the pion exchange. When introducing the short range correlation in the K exchange, one obtains the p-wave effective interaction of $\Lambda N \to NN$:

$$G^{K,\mathrm{p-wave}}_{\Lambda N\to NN}(q) = [V'_{l,K}(q)\hat{q}_i\hat{q}_j + V'_{t,K}(q)(\delta_{ij} - \hat{q}_i\hat{q}_j)]\sigma_i^{(1)}\sigma_j^{(2)}C_P^{K,N} \tag{31}$$

with

$$V'_{l,K}(q) = -\frac{f_{K\Lambda N}}{\mu}\frac{P}{\mu}[\vec{q}^2 D_K(q)F_K^2(q) + g^{\Lambda}_{l,K}(q)] \tag{32}$$

$$V'_{t,K}(q) = -\frac{f_{K\Lambda N}}{\mu}\frac{P}{\mu}g^{\Lambda}_{t,K}(q) \tag{33}$$

and the parity violating part is written as

$$G^{K,\mathrm{s-wave}}_{\Lambda N\to NN}(q) = V'_{s,K}(q)\ \hat{q}_i\ \sigma_i^{(1)}\ C_S^{K,N} \tag{34}$$

with

$$V'_{s,K}(q) = -\frac{f_{K\Lambda N}}{\mu}S[D_K(q)F_K^2(q) + g^{\Lambda}_{s,K}(q)]|\vec{q}| \tag{35}$$

Here $D_K(q)$ is the propagator for K and the form factor for K is defined as

$$F_K(q) = \frac{\Lambda_K^2}{\Lambda_K^2 - q^2} \tag{36}$$

with $\Lambda_K = \Lambda_\pi = 1.0$ GeV.

In order to introduce one K exchange in the previous results, we replace the π propagator by the $\pi + K$ with the following rules:

$$\begin{array}{lrcrcl} \text{proton} & \pi^0: & -V'_{l,t} & \longrightarrow & \pi^0 + \bar{K}^0: & -V'_{l,t} + C_P^{\bar{K}^0 p}V'_{l,t,K} \\ & \pi^-: & 2V'_{l,t} & \longrightarrow & \pi^- + K^-: & 2V'_{l,t} + C_P^{K^- p}V'_{l,t,K} \\ \text{neutron} & \pi^0: & V'_{l,t} & \longrightarrow & \pi^0 + \bar{K}^0: & V'_{l,t} + C_P^{\bar{K}^0 n}V'_{l,t,K} \end{array} \tag{37}$$

while in s-wave part of the exchange we replace:

$$\begin{array}{lrcrcl} \text{proton} & \pi^0: & -V'_s\sigma_i^{(2)}\hat{q}_i & \longrightarrow & \pi^0 + \bar{K}^0: & -V'_s\sigma_i^{(2)}\hat{q}_i + C_S^{\bar{K}^0 p}V'_{s,K}\sigma_i^{(1)}\hat{q}_i \\ & \pi^-: & 2V'_s\sigma_i^{(2)}\hat{q}_i & \longrightarrow & \pi^- + K^-: & 2V'_s\sigma_i^{(2)}\hat{q}_i + C_S^{K^- p}V'_{s,K}\sigma_i^{(1)}\hat{q}_i \\ \text{neutron} & \pi^0: & V'_s\sigma_i^{(2)}\hat{q}_i & \longrightarrow & \pi^0 + \bar{K}^0: & V'_s\sigma_i^{(2)}\hat{q}_i + C_S^{\bar{K}^0 n}V'_{s,K}\sigma_i^{(1)}\hat{q}_i \end{array} \tag{38}$$

In the direct terms of s-wave (see fig. 6 (d))the pion cannot interfere with K, because the spin sum vanishes in the nucleon loop.

The results with one pion and one K exchange in the lowest order of the RPA series are the following ones:

$$\begin{aligned} T_p^{\pi+K,\mathrm{s-wave}}(q) &= 5V_s'^2 + (V'_{s,K}C_S^{\bar{K}^0,p})^2 + (V'_{s,K}C_S^{K^-,p})^2 \\ &\quad +(-V_s' + V'_{s,K}C_S^{\bar{K}^0,p})(2V_s' + V'_{s,K}C_S^{K^-,p}) \end{aligned} \tag{39}$$

$$\begin{aligned} T_p^{\pi+K,\mathrm{p-wave}}(q) &= (-V_l' + V'_{l,K}C_P^{\bar{K}^0,p})^2 + (2V_l' + V'_{l,K}C_P^{K^-,p})^2 \\ &\quad +2\{(-V_t' + V'_{t,K}C_P^{\bar{K}^0,p})^2 + (2V_t' + V'_{t,K}C_P^{K^-,p})^2\} \\ &\quad -(-V_l' + V'_{l,K}C_P^{\bar{K}^0,p})(2V_l' + V'_{l,K}C_P^{K^-,p}) \\ &\quad +2(-V_l' + V'_{l,K}C_P^{\bar{K}^0,p})(2V_t' + V'_{t,K}C_P^{K^-,p}) \\ &\quad +2(2V_l' + V'_{l,K}C_P^{K^-,p})(-V_t' + V'_{t,K}C_P^{\bar{K}^0,p}) \end{aligned} \tag{40}$$

$$\begin{aligned} T_n^{\pi+K,\mathrm{s-wave}}(q) &= V_s'^2 + (V'_{s,K}C_S^{\bar{K}^0,n})^2 \\ &\quad +\frac{1}{2}(V_s' + V'_{s,K}C_S^{\bar{K}^0,n})^2 \end{aligned} \tag{41}$$

$$\begin{aligned} T_n^{\pi+K,\mathrm{p-wave}}(q) &= (V_l' + V'_{l,K}C_P^{\bar{K}^0,n})^2 + 2(V_t' + V'_{t,K}C_P^{\bar{K}^0,n})^2 \\ &\quad -\frac{1}{2}(V_l' + V'_{l,K}C_P^{\bar{K}^0,n})^2 \\ &\quad +2(V_l' + V'_{l,K}C_P^{\bar{K}^0,n})(V_t' + V'_{t,K}C_P^{\bar{K}^0,n}) \end{aligned} \tag{42}$$

In order to include all orders of the RPA series, we just replace

$$\begin{aligned} V_{i,(1)}'^2 &\rightarrow \frac{V_{i,(1)}'^2}{|1 - UV_i|^2} \\ V'_{l,(1)}V'_{t,(2)} + V'_{l,(2)}V'_{t,(1)} &\rightarrow \mathrm{Re}\left\{\frac{1}{1-UV_l}\frac{1}{1-U^*V_t}\right\}(V'_{l,(1)}V'_{t,(2)} + V'_{l,(2)}V'_{t,(1)}) \end{aligned} \tag{43}$$

Here $V'_{i,(1)}$ and $V'_{i,(2)}$ with $i = l, t, s$ stand for the effective interactions with π or K exchange. The s-wave component of K, however, remains $V_{s,K}'^2$, because the vertex in the Kph excitation contains no $\vec{\sigma}$ and hence this ph excitation does not get modified by the effective strong spin-isospin interaction.

4 Two-pion exchange

Another kind of diagrams that have been traditionally studied are those corresponding to two-pion exchange. We will divide the study of these diagrams into two categories: correlated two-pion exchange and uncorrelated two-pion exchange. In the case of correlated exchange we will only consider the scalar-isoscalar channel, where the σ meson appears. The vector channel is neglected since the ρ contribution has been seen to be not relevant [15, 32]. Simple estimations will also be done here. We will also see that the scalar-isoscalar channel is also the relevant one in the case of uncorrelated two-pion exchange. The effect of heavier scalar mesons (such as the f_0, a_0) is also negligible [15].

4.1 Correlated two-pion exchange

Some works on this topic have been done [14, 15, 33], incorporating the σ meson as an explicit degree of freedom. There it is found that, working with reasonable values for the mass, width and $\sigma\pi\pi$ coupling, the role of this "$2\pi/\sigma$" exchange is relevant in the non-mesonic decay problem.

A less phenomenological treatment of the sigma meson is provided by Chiral Unitary Approaches [28, 34, 35, 36, 37]. In [28] it was found that the σ meson is dynamically generated by the interaction of two pion in flight when summing up the s-wave $t-$matrix of the $\pi\pi$ scattering to all orders using the Bethe-Salpeter equation. The former picture of the σ meson was used to describe its role in the NN interaction in ref. [26], finding a moderate attraction beyond $r = 0.9$ fm and a repulsion at shorter distances, in contrast with the attraction of the conventional σ exchange. We will follow an analogous model to the one of the aforementioned reference.

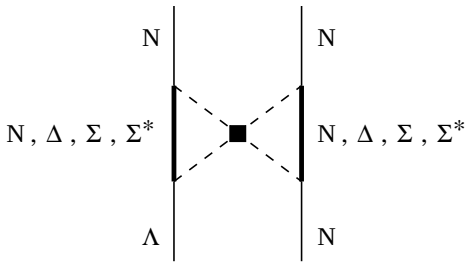

Figure 7: Diagrams corresponding to the correlated two-pion exchange, with in-flight interaction of the two mesons.

The diagrams corresponding to the correlated exchange are those of fig. (7). In the weak vertex we will only consider at the moment the parity conserving term of the Lagrangians (we will see later that the contribution from the parity violating part is not relevant). This simplifies the problem because, as the parity conserving part (proportional to $\vec{\sigma}\vec{q}$, where $\vec{q}$ is the momentum of the pion) has the same structure as the strong πNN vertex, the results obtained in ref. [26] are also applicable here. In that reference it was shown that there is a cancellation of the meson-meson vertex off-shell part of the diagram 8A with the diagrams 8B containing a $\pi\pi\pi NN$ vertex. Taking this fact into account, the rescattering of the pions

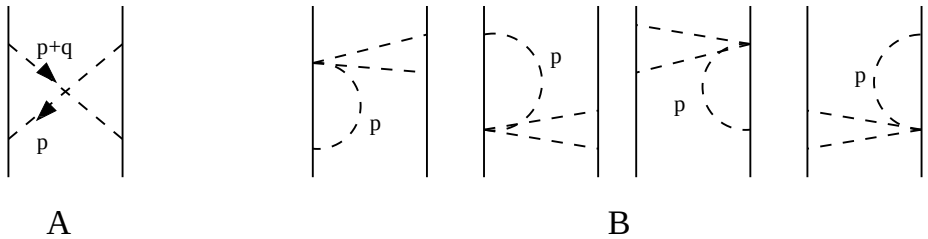

Figure 8: Diagrams where the off-shell cancellations appear. The off-shell part of the pion lines in diagram A cancels diagrams B.

can be treated non-perturbatively by means of the Bethe-Salpeter equation, as was done in ref. [28]. Such a treatment also applies in the case of the $\Lambda N \to NN$ interaction when considering only the parity conserving term of the interacting Lagrangian. One is then allowed to take the expression of the potential coming from the diagrams with N and Δ as

intermediate states from that reference, with the only difference of a multiplicative factor $\mathfrak{R}$ that reflects the replacement of one strong πNN vertex by the weak $\Lambda\pi N$. The potential is then given by [26]:

$$V_{corr}^{2\pi}(q) = \mathfrak{R}\ v^2(q)\frac{6}{f^2}\frac{\vec{q}^{\,2}+\frac{\mu^2}{2}}{1-G(-\vec{q}^{\,2})\left(\vec{q}^{\,2}+\frac{\mu^2}{2}\right)\frac{1}{f^2}} \tag{44}$$

where $G(s)$ is the loop function with two pion propagators, and $v(q)$ (associated to diagrams of fig. 7 with intermediate N, Δ) and $\mathfrak{R}$ are given by:

$$\begin{aligned}\mathfrak{R} &= \frac{P/\mu}{\frac{D+F}{2f}}\\ v(q) &= v_N(q)+v_\Delta(q)\end{aligned} \tag{45}$$

In the former equation $v_N(q)$ can be written, after performing the p^0 integration and assuming that the Λ baryon is initially at rest, as:

$$\begin{aligned}v_N(q) = \int \frac{d^3p}{(2\pi)^3}\left(\frac{D+F}{2f}\right)^2(\vec{p}^{\,2}+\vec{p}\cdot\vec{q})\frac{M_N}{2E_N}\frac{1}{\omega}\frac{1}{\omega'}\theta(|\vec{p}|-k_F)\frac{1}{\omega+\omega'}\\ \times\frac{1}{E_N+\omega-M_\Lambda}\ \frac{1}{E_N+\omega'-M_\Lambda}(\omega+\omega'+E_N-M_\Lambda)\end{aligned} \tag{46}$$

In the former equations the momenta $\vec{p}$ and $\vec{q}$ are those of fig. (8) and:

$$E=E(\vec{p});\qquad \omega=\sqrt{\mu^2+\vec{p}^{\,2}};\qquad \omega'=\sqrt{\mu^2+(\vec{p}+\vec{q})^{\,2}}. \tag{47}$$

θ is the Heaviside function and k_F is the Fermi momentum. In eq. (46) we have neglected the energy transfer q^0 which is small compared with $\vec{q}$.

The $v_\Delta(q)$ function has the same structure as $v_N(q)$. The only difference is that we have to replace the energy and the mass of the intermediate nucleon by those of the Δ, and the πNN vertex by the $\pi N\Delta$ one. The Heaviside function disappears now from the integrand since the Δ resonance is not Pauli-blocked, and there is also an extra isospin coefficient:

$$\begin{aligned}v_\Delta(q) = \frac{4}{9}\left(\frac{f_{\pi N\Delta}}{f_{\pi NN}}\right)^2\left(\frac{D+F}{2f}\right)^2\int\frac{d^3p}{(2\pi)^3}(\vec{p}^{\,2}+\vec{p}\cdot\vec{q})\frac{M_\Delta}{2E_\Delta}\frac{1}{\omega}\frac{1}{\omega'}\frac{1}{\omega+\omega'}\\ \times\frac{1}{E_\Delta+\omega-M_\Lambda}\ \frac{1}{E_\Delta+\omega'-M_\Lambda}(\omega+\omega'+E_\Delta-M_\Lambda)\end{aligned} \tag{48}$$

Here $f_{\pi N\Delta}$ parameterizes the $\pi N\Delta$ coupling, with $f_{\pi N\Delta}=2.12\ f_{\pi NN}$. The regularization of these loops can be accomplished by means of a form factor. We take static form factors as in [26]:

$$F(\vec{p})F(\vec{p}+\vec{q}) = \frac{\Lambda_\pi^2}{\Lambda_\pi^2+\vec{p}^{\,2}}\ \frac{\Lambda_\pi^2}{\Lambda_\pi^2+(\vec{p}+\vec{q})^2} \quad , \tag{49}$$

and in our calculations we take Λ_π=1 GeV.

So far we have been studying diagrams in which the Λ baryon appears in the weak vertices. However, as we can see in fig. 7, there are also diagrams with a strange intermediate baryon (Σ, Σ^*) strongly coupled to the Λ. In these new diagrams the cancellation of the meson-meson vertex off-shell part of diagram 8A with the diagrams 8B also holds. Therefore, we only need to calculate the $v_\Sigma(q)$ and $v_{\Sigma^*}(q)$ functions (analogous to $v_N(q)$ and $v_\Delta(q)$) which correspond to the diagrams depicted in fig. 9. In order to calculate these functions we need to know the $\Lambda\Sigma\pi$, $\Lambda\Sigma^*\pi$, $\Sigma N\pi$ and $\Sigma^* N\pi$ vertices (see fig. 10).

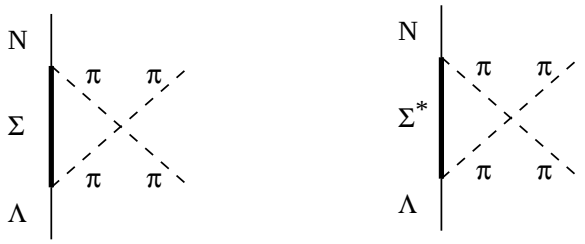

Figure 9: The two pion correlated exchange triangle vertex through Σ and Σ^* excitations.

The strong $\Lambda\Sigma\pi$ vertex is given in ref. [38] and the $\Lambda\Sigma^*\pi$ vertex can be obtained from the former one by replacing the spin and isospin Pauli matrices by the analogous representation-changing operators $\vec{S}$ and $\vec{T}$ and by invoking $SU(6)$ symmetry, as done in [39]. We can write the strong $\Lambda\Sigma\pi$ and $\Lambda\Sigma^*\pi$ vertices as:

$$\begin{aligned} -it_{\Lambda\Sigma\pi} &= \frac{1}{\sqrt{3}}\frac{D}{f}\vec{\sigma}\cdot\vec{q} \\ -it_{\Lambda\Sigma^*\pi} &= \frac{6}{5}\frac{D+F}{2f}\vec{S}\cdot\vec{q} \end{aligned} \tag{50}$$

for an incoming pion of momentum $\vec{q}$.

The calculation of the weak $\Sigma N\pi$ and $\Sigma^* N\pi$ vertices is not so trivial. Here we only care about the parity conserving part of these vertices, as said before. As commented in the former section one cannot use current algebra arguments and must resort to some model. Here we take a simple one using $SU(3)$ symmetry plus the $\Delta I = 1/2$ rule. We implement this rule by introducing in the initial state a fictitious $|1/2\ 1/2; 1\rangle \equiv \bar{K}^0$ state, which we couple to the nucleon, and then we couple the resulting state to the pion to get the Σ (Σ^*) baryon. Experimental values for the $\Sigma N\pi$ couplings (both for the parity conserving and parity violating parts) and some constraints can be found in reference [12]. Our results satisfy the aforementioned constraints since they come from $SU(2)$ symmetry plus $\Delta I = 1/2$ rule, and therefore are also valid for the $\Sigma^* N\pi$ couplings. We get also a reasonable good agreement with the experimental data and this is enough because, as we are going to see, there are big cancellations between the diagrams with an intermediate Σ and those with an intermediate Σ^*, and the final results barely depend on the inclusion of these diagrams in the calculations. In fact, in our final results we will neglect these diagrams.

We get for the weak vertex of the diagrams of fig. 10:

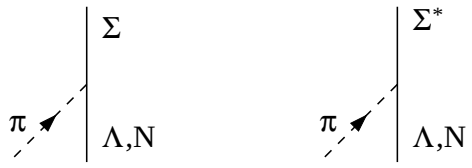

Figure 10: Vertices needed to evaluate the $v_\Sigma(q)$ and $v_{\Sigma^*}(q)$ functions.

$$-it_{\Sigma N\pi} = \Re(a_\Sigma d + b_\Sigma f)\vec{\sigma}\cdot\vec{q} \qquad -it_{\Sigma^* N\pi} = \Re a_{\Sigma^*} d\vec{S}^\dagger\cdot\vec{q} \tag{51}$$

where the values of a_Σ, b_Σ and a_{Σ^*} are given in table 4.1.

	$\pi^- p$	$\pi^0 p$	$\pi^- n$	$\pi^0 n$	$\pi^+ n$
a_Σ	0	0	-1/$\sqrt{10}$	-1/$\sqrt{10}$	-1/$\sqrt{10}$
b_Σ	-1/$\sqrt{3}$	1/$\sqrt{3}$	-1/$\sqrt{6}$	0	1/$\sqrt{6}$
a_{Σ^*}	$\frac{3\sqrt{2}}{5\sqrt{15}}$	$-\frac{3\sqrt{2}}{5\sqrt{15}}$	$\frac{3}{5\sqrt{15}}+\frac{3}{5\sqrt{5}}$	$\frac{3}{5\sqrt{5}}$	$-\frac{3}{5\sqrt{15}}+\frac{3}{5\sqrt{5}}$

Table 2: Values of the coefficients of eq. (51) for the parity conserving part of the weak vertex.

With these values for the $\Sigma N\pi$ and $\Sigma^* N\pi$ couplings we can finally calculate the $v_\Sigma(q)$ and $v_{\Sigma^*}(q)$ functions. We obtain:

$$\begin{aligned} v_\Sigma(q) &= \int \frac{d^3p}{(2\pi)^3}\frac{D}{\sqrt{3}f}\left(\frac{D+F}{2f}\right)(\vec{p}^{\,2}+\vec{p}\cdot\vec{q})\frac{M_\Sigma}{2E_\Sigma}\frac{1}{\omega\omega'}\;\frac{1}{\omega+\omega'} \\ &\quad\times\frac{1}{E_\Sigma+\omega-M_\Lambda}\;\frac{1}{E_\Sigma+\omega'-M_\Lambda}(\omega+\omega'+E_\Sigma-M_\Lambda) \\ v_{\Sigma^*}(q) &= -\int \frac{d^3p}{(2\pi)^3}\frac{12\sqrt{2}}{25}\left(\frac{D+F}{2f}\right)^2(\vec{p}^{\,2}+\vec{p}\cdot\vec{q})\frac{M_{\Sigma^*}}{2E_{\Sigma^*}}\frac{1}{\omega\omega'}\;\frac{1}{\omega+\omega'} \\ &\quad\times\frac{1}{E_{\Sigma^*}+\omega-M_\Lambda}\;\frac{1}{E_{\Sigma^*}+\omega'-M_\Lambda}(\omega+\omega'+E_{\Sigma^*}-M_\Lambda) \end{aligned} \tag{52}$$

where the notation followed is the same as in eq (46). We can see that $v_\Sigma(q)$ and $v_{\Sigma^*}(q)$ have opposite sign, thus leading to the aforementioned cancellation.

At this point we have all the ingredients to calculate the $V^{2\pi}_{corr}(q)$ of equation eq (44) corresponding to the correlated two-pion exchange. The only thing one has to do is to generalize the definition of $v(q)$ of eq. (45) by:

$$v(q) = v_N(q) + v_\Delta(q) + v_\Sigma(q) + v_{\Sigma^*}(q) \tag{53}$$

In fig. 11 we plot $V^{2\pi}_{corr}(q)$ both with and without considering the diagrams with intermediate Σ, Σ^*. As we can see, the effect of these latter diagrams is very small due to the cancellation between them. In our calculations we will no longer include these diagrams.

In order to include the short range correlations we will use $V^{2\pi}_{corr}(q) - \widetilde{V}^{2\pi}_{corr}(q)$ instead of $V^{2\pi}_{corr}(q)$, where the tilde on the function means that $\vec{q}^{\,2}$ must be replaced by $\vec{q}^{\,2}+q_c^2$, being q_c the inverse of a typical correlation length (see Appendix).

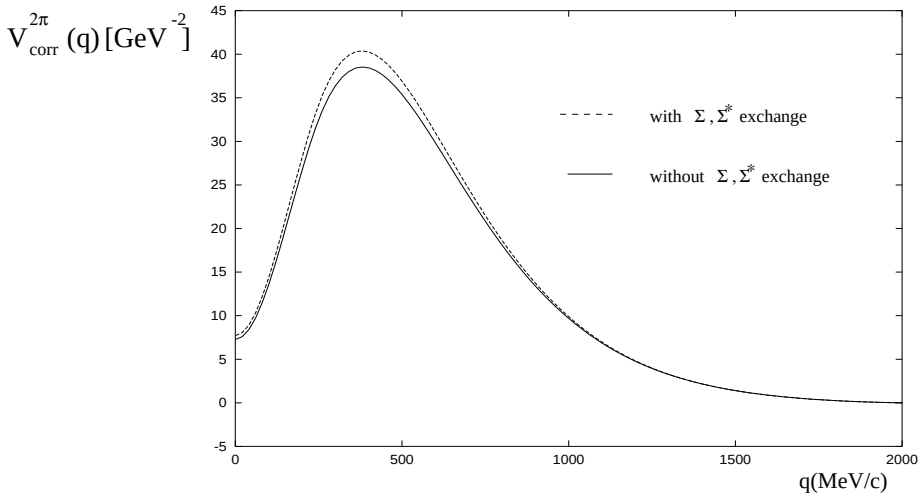

Figure 11: The $V^{2\pi}_{corr}(q)$ function corresponding to the correlated two-pion exchange with and without including the Σ, Σ^* exchange diagrams, before multiplying by the $\mathfrak{R}$ factor.

4.2 Uncorrelated two-pion exchange

The other set of processes that we have to study when considering the two-pion exchange is the one in which the exchanged pions only interact with baryonic legs and not with other pions (uncorrelated exchange). The corresponding Feynman diagrams are depicted in fig. 12.

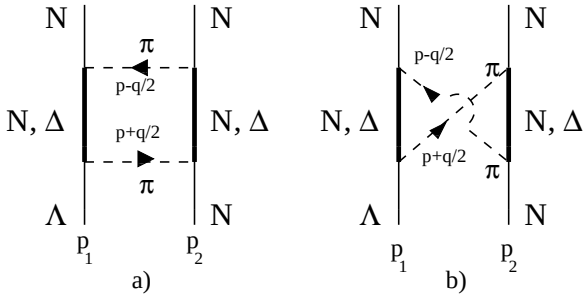

Figure 12: The two pion uncorrelated exchange triangle vertex through N and Δ excitations.

We do not include the diagrams with an intermediate Σ and Σ^*, because one expects a similar cancellation to the one found in the correlated exchange, nor the diagrams with two nucleon propagators in diagram 12 (a), which correspond to final state interaction and are included in the correlations. We will neglect also the spin dependent term, which is found to be of order $2q^2/(9p^2)$ with respect to the spin-independent one. Here q is the momentum transfer and p is the loop variable, which is cut around 1GeV by the cut off, so taking $\langle p \rangle \sim 800$ MeV/c and $q \sim 400$ MeV/c we find $2q^2/(9p^2) \sim 6\%$, and therefore we do not care about it.

Let us consider first the direct exchange. As an example we write the contribution of the diagram with one intermediate nucleon in the left hand baryonic line of fig. 12 (a), and an intermediate Δ in the right one. We will include at the end the factor $\mathfrak{R}$ associated to the weak vertex. The modifications needed to describe the other diagrams are trivial. The potential associated to the aforementioned exchange is:

$$-iv^{dir}_{N\Delta}(q) = \int \frac{d^4p}{(2\pi)^4} \frac{M_N}{E(\vec{p_1}-\vec{p}-\vec{q}/2)} \frac{M_\Delta}{E_\Delta(\vec{p_2}+\vec{p}+\vec{q}/2)} \frac{i\ (1-n(\vec{p_1}-\vec{p}-\vec{q}/2))}{p_1^0-p^0-q^0/2-E(\vec{p_1}-\vec{p}-\vec{q}/2)+i\epsilon}$$
$$\times \frac{i}{p_2^0+p^0+q^0/2-E_\Delta(\vec{p_2}+\vec{p}+\vec{q}/2)+i\epsilon} \frac{i}{(p+q/2)^2-\mu^2+i\epsilon} \frac{i}{(p-q/2)^2-\mu^2+i\epsilon} \left(\frac{f_{\pi NN}}{\mu}\right)^2$$
$$\times \left(\frac{f_{\pi\Delta N}}{\mu}\right)^2 \vec{\sigma_1}\cdot(\vec{p}-\vec{q}/2)\ \vec{\sigma_1}\cdot(\vec{p}+\vec{q}/2)\ \vec{S_2}\cdot(\vec{p}-\vec{q}/2)\ \vec{S_2}^{\dagger}\cdot(\vec{p}+\vec{q}/2)\tau_1^i\tau_1^j T_2^i T_2^{\dagger j} \tag{54}$$

where $\vec{S}$ and $\vec{T}$ are the spin and isospin transition operators normalized such that they satisfy:

$$S_i S_j^\dagger = \frac{2}{3}\delta_{ij} - \frac{i}{3}\epsilon_{ijk}\sigma_k$$
$$T_i T_j^\dagger = \frac{2}{3}\delta_{ij} - \frac{i}{3}\epsilon_{ijk}\tau_k \tag{55}$$

To regularize these loops we will include a cutoff in the space of intermediate states together with static form factors in the πNN vertices, as done in the case of correlated two pion exchange. We will also work with the initial Λ and nucleon at rest in order to simplify the calculations.

The calculation of the crossed exchange is analogous. As before, we will write the contribution of the diagram containing one nucleon propagator in the left baryonic line of fig.12.b, and a Δ propagator in the right one:

$$-iv^{cross}_{N\Delta}(q) = \int \frac{d^4p}{(2\pi)^4} \frac{M_N}{E(\vec{p_1}-\vec{p}-\vec{q}/2)} \frac{M_\Delta}{E_\Delta(\vec{p_2}-\vec{p}+\vec{q}/2)} \frac{i\ (1-n(\vec{p_1}-\vec{p}-\vec{q}/2))}{p_1^0-p^0-q^0/2-E(\vec{p_1}-\vec{p}-\vec{q}/2)+i\epsilon}$$
$$\times \frac{i}{p_2^0-p^0+q^0/2-E_\Delta(\vec{p_2}-\vec{p}+\vec{q}/2)+i\epsilon} \frac{i}{(p+q/2)^2-\mu^2+i\epsilon} \frac{i}{(p-q/2)^2-\mu^2+i\epsilon} \left(\frac{f_{\pi NN}}{\mu}\right)^2$$
$$\times \left(\frac{f_{\pi\Delta N}}{\mu}\right)^2 \vec{\sigma_1}\cdot(\vec{p}-\vec{q}/2)\ \vec{\sigma_1}\cdot(\vec{p}+\vec{q}/2)\ \vec{S_2}\cdot(\vec{p}-\vec{q}/2)\ \vec{S_2}^{\dagger}\cdot(\vec{p}+\vec{q}/2)\tau_1^i\tau_1^j T_2^i T_2^{\dagger j} \tag{56}$$

The regularization is achieved also by including a cutoff and static form factors. The p^0 integral can be analytically performed in both cases.

The resulting uncorrelated two-pion exchange potential can be divided into an isoscalar and an isovector piece:

$$V^{2\pi}_{unc}(q) = V^{2\pi}_{is,unc}(q) + V^{2\pi}_{iv,unc}(q)\vec{\tau}\cdot\vec{\tau} \tag{57}$$

where these two pieces are:

$$V^{2\pi}_{is,unc}(q) = 3\Re v^{cross}_{NN}(q) + \frac{4\Re}{3}\left(v^{dir}_{\Delta N}(q) + v^{dir}_{N\Delta}(q) + v^{cross}_{\Delta N}(q) + v^{cross}_{N\Delta}(q)\right) + \frac{16\Re}{27}\left(v^{dir}_{\Delta\Delta}(q) + v^{cross}_{\Delta\Delta}(q)\right)$$
$$V^{2\pi}_{iv}(q) = 2\Re v^{cross}_{NN}(q) + \frac{4\Re}{9}\left(v^{dir}_{\Delta N}(q) + v^{dir}_{N\Delta}(q) - v^{cross}_{\Delta N}(q) - v^{cross}_{N\Delta}(q)\right) + \frac{8\Re}{81}\left(v^{cross}_{\Delta\Delta}(q) - v^{dir}_{\Delta\Delta}(q)\right) \tag{58}$$

It is worth mentioning that, as we are not taking into account direct diagrams with two nucleon propagators, $V^{2\pi}_{unc}(q)$ is real. The isoscalar and isovector parts of the function of eq. (58) are plotted in fig. 13. As we can see there, the isoscalar part is dominant around $q \sim 420$ MeV/c, so from now on we will neglect the isovector contribution. This simplifies the description since the remaining scalar-isoscalar contribution can be added directly to the correlated "$2\pi/\sigma$" exchange of the previous subsection. As in the correlated exchange case, short range correlations must be taken into account and their inclusion is achieved, as before, by subtracting to $V^{2\pi}_{is,unc}(q)$ its value at $\vec{q}^{\,2} + q_c^2$ (see Appendix).

Up to now we have not taken into account the parity violating part of the weak vertex in the two-pion exchange contributions. We have evaluated this contribution both in the correlated and uncorrelated two-pion exchange and we find these terms small. Additionally there is a cancellation between them, so the inclusion of this term is irrelevant. The point is that one cannot have an intermediate Δ coupled to the Λ in the weak vertex, and this reduces the correlated exchange contribution to 1/5 of the one of the parity conserving part but also reduces strongly the contribution of the uncorrelated exchange, leading to a very big cancellation at the relevant momentum $q \sim 420$ MeV/c. The structure of these terms is exactly the same as the (s-wave) parity violating term in the K exchange and their summed strength is found negligible compared to this latter term.

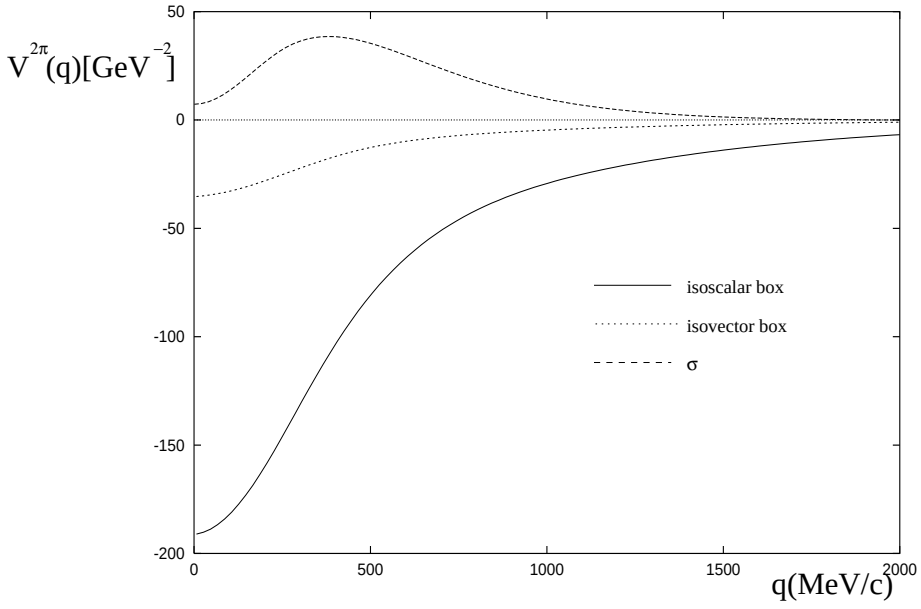

Figure 13: Isoscalar and isovector pieces of the uncorrelated two-pion exchange potential and the σ (correlated 2π exchange) potential (without including the factor $\mathfrak{R}$).

The inclusion of the two-pion scalar-isoscalar terms is easy. These terms only have interferences with the p-wave part of the $\pi + K$ exchange. By using eqs. (44) and (58) we define:

$$V'_{2\pi}(q) = \frac{V^{2\pi}_{corr}(q) + V^{2\pi}_{is,unc}(q)}{\mathfrak{R}} \tag{59}$$

and the new contributions are accounted for by adding to eqs. (39) to (42) the following terms:

$$
\begin{aligned}
T^{2\pi}_{p,S}(q) &= (V'_{2\pi}(q))^2 \\
T^{2\pi}_{p,P,int}(q) &= -V'_{2\pi}(q)(2V_l' + V'_{l,K}C_P^{K^-p})\mathrm{Re}\left(\frac{1}{1-UV_l}\right) \\
&\quad - V'_{2\pi}(q)(4V_t' + 2V'_{t,K}C_P^{K^-p})\mathrm{Re}\left(\frac{1}{1-UV_t}\right) \\
T^{2\pi}_{n,S}(q) &= \frac{1}{2}(V'_{2\pi}(q))^2 \\
T^{2\pi}_{n,P,int}(q) &= -V'_{2\pi}(q)(V_l' + V'_{l,K}C_P^{\bar{K}^0n})\mathrm{Re}\left(\frac{1}{1-UV_l}\right) \\
&\quad - V'_{2\pi}(q)(2V_t' + 2V'_{t,K}C_P^{\bar{K}^0n})\mathrm{Re}\left(\frac{1}{1-UV_t}\right)
\end{aligned}
\tag{60}
$$

The repulsive character of our correlated two-pion exchange in momentum space is somewhat unexpected but it is linked to an important constraint of chiral symmetry, i.e., the Adler zero at $s = \mu^2/2$ where the $\pi\pi$ scalar-isoscalar amplitude changes sign. In coordinate space it leads to a moderate attraction at intermediate and long distances, and to a repulsion at short distances [26]. Such repulsion from the correlated two-pion exchange is actually not so novel and in models like the Skyrme model, where only pion degrees of freedom are considered, the scalar-isoscalar NN interaction also shows repulsion at short distances [40]. However, it is worth noting that when we sum the correlated and uncorrelated two-pion contribution we obtain a net attraction in coordinate space. This is shown in fig. 14.

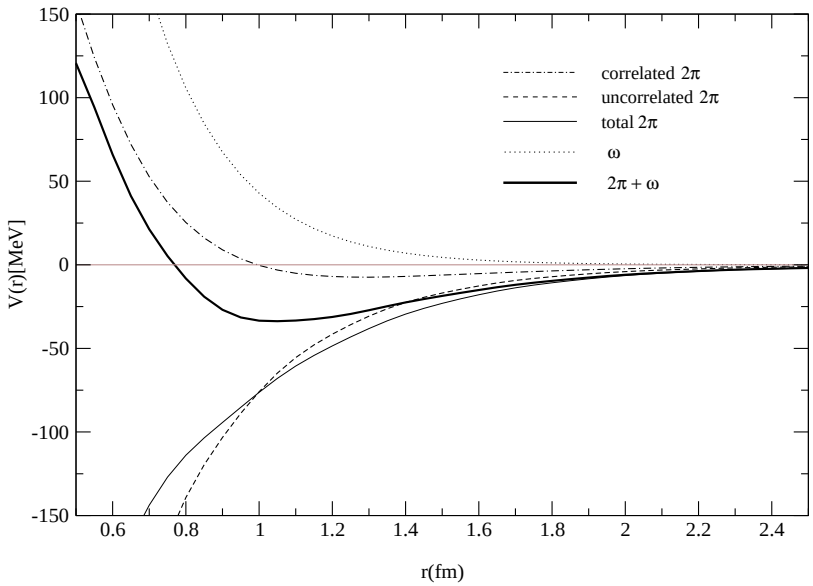

Figure 14: Central potentials of the strong NN interaction in coordinate space from correlated two-pion (dashed-dotted line), uncorrelated two-pion (dashed line) and omega meson (dotted line) exchanges. The thick solid and thin solid lines denote the sum of all contributions and the sum without the omega meson, respectively.

Once at this point, we would also like to connect our results with present realistic forces of the NN interactions. We choose the Argonne potentials v_{14}, v_{18} [41] (see also the paper [42] for a discussion of this central potential). We observe that this potential has a moderate attraction of around 20-30 MeV at intermediate distances and becomes repulsive at short distances. Our potential with correlated plus uncorrelated two-pion exchange is only attractive. Obviously other contributions are missing there, and the conventional meson exchange approach to generate this repulsion is the ω exchange. We thus add the omega exchange to our potential and find that for standard values of the coupling and the form factor we can reproduce fairly well the Argonne v_{14} potential. This is seen in fig. 14, where we have chosen the coupling $g_\omega = 13$ and $\Lambda_\omega = 1.4$ GeV, for a monopole form factor.

Now we turn to the weak interaction. Since we have seen that ω exchange plays a role in the strong interaction, we would also like to include it in the weak transition. For this purpose we take the strong coupling determined here from the NN central potential and use the weak coupling of the ω given in [2] $g^W_{\Lambda N\omega} = 3.69 G\mu^2$ (for the parity conserving part, and the sign is the same one as for the weak parity conserving pion coupling), and same form factor as for the strong vertex. With the sign prescription for our strong and weak Lagrangians this ω potential in momentum space is given by

$$V_\omega(\vec{q}) = \frac{g^W_{\Lambda N\omega} g_\omega}{\vec{q}^{\,2} + m_\omega^2} \left(\frac{\Lambda_\omega^2 - m_\omega^2}{\Lambda_\omega^2 + \vec{q}^{\,2}} \right)^2 \tag{61}$$

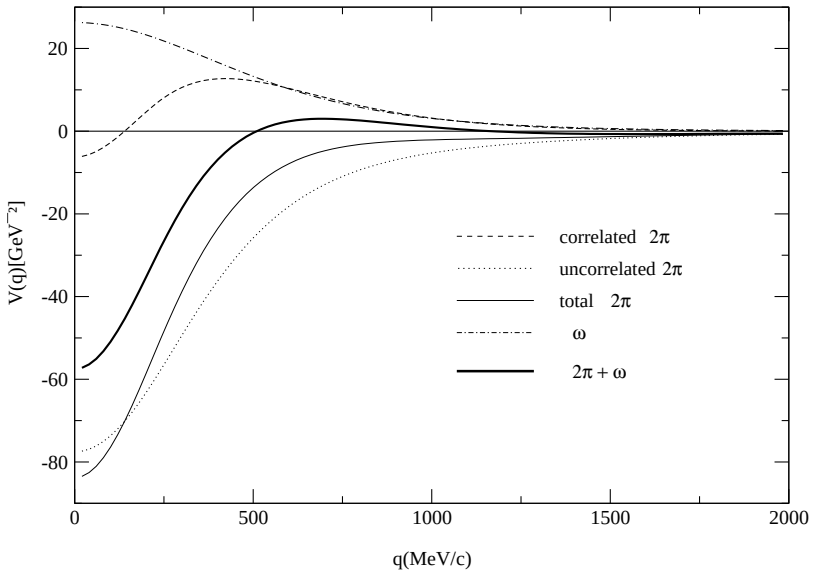

Figure 15: Weak transition potentials in momentum space (divided by $G\mu^2$) from correlated two-pion (dashed line), uncorrelated two-pion (dotted line) and omega meson (dotted-dashed line) exchanges. The thick solid and thin solid lines denote the sum of all contributions and the sum without the omega meson, respectively. Here we have multiplied by the factor $\mathfrak{R}$ both the correlated and uncorrelated two-pion exchange, and we have already included the effect of short range correlations by subtracting to the potentials their values at $\vec{q}^{\,2} + q_c^2$.

In fig. 15 we show now our results for the transition potential in momentum space for the weak two-pion exchange, omega exchange and their sum. We observe that around

$q = 400$MeV/c the inclusion of the ω exchange reduces the contribution of the scalar-isoscalar transition to about 30% of the contribution of the two-pion exchange alone. We shall discuss the effect of the ω exchange in the results for the total decay widths and Γ_n/Γ_p ratio in the next section.

5 Results

We show the results for the proton and neutron induced decay widths of ${}^{12}_{\Lambda}$C separating the different contributions. In table 3 we show the results obtained with only one pion exchange. In table 4 we show the results with only one kaon exchange and only the scalar-isoscalar two-pion exchange. In table 5 we show the different interference terms and in table 6 the results obtained including $\pi + K$, $\pi + K + 2\pi$ and $\pi + K + 2\pi + \omega$.

	S	P_L	P_T	$P_{int.\ LT}$	Total
$\Gamma_p/\Gamma_\Lambda^{free}$	0.177	0.684	0.012	0.082	0.956
$\Gamma_n/\Gamma_\Lambda^{free}$	0.089	0.049	0.003	-0.021	0.119

Table 3: OPE contributions to Γ_p and Γ_n: s-wave, longitudinal p-wave, transverse p-wave and interference between longitudinal and transverse p-wave. Decay rates given in units of the free Λ width.

	S	P_L	P_T	$P_{int.\ LT}$	Total kaon	2π
$\Gamma_p/\Gamma_\Lambda^{free}$	0.058	0.152	0.012	0.030	0.253	0.191
$\Gamma_n/\Gamma_\Lambda^{free}$	0.110	0.022	0.005	-0.019	0.118	0.095

Table 4: One kaon exchange and two pion exchange contributions to the partial decay widths.

	πK_S	πK_L	πK_T	πK_{LT}	"σ"π_L	"σ"π_T	"σ"K_L	"σ"K_T
$\Gamma_p/\Gamma_\Lambda^{free}$	0.075	-0.629	-0.024	-0.109	-0.264	0.057	0.126	-0.060
$\Gamma_n/\Gamma_\Lambda^{free}$	0.065	-0.064	-0.007	0.042	-0.132	0.029	0.082	-0.039

Table 5: Interferences between the different contributions. Here "σ" means two pion exchange, both correlated and uncorrelated.

While K or 2π contributions by themselves are small compared to Γ_p from OPE, the interference effects with the OPE contribution are large. As we can see from table 5, one of the important pieces of interference is in the longitudinal part of the p-wave contribution. The kaon exchange produces a large cancellation of this contribution from OPE in Γ_p. The interference of 2π exchange and OPE in the p-wave longitudinal channel is also relevant, and to a smaller extend also the interference of 2π with K exchange.

If one looks at table 5 and compares it to table 3 one can see that the main effect of the K exchange contribution is to decrease the p-wave contribution of the OPE in the proton case, which was responsible for the large Γ_n/Γ_p ratio. The two-pion exchange contribution

	π	$\pi+K$	$\pi+K+$"σ"	$\pi+K+$"σ"$+\omega$
$\Gamma_p/\Gamma_\Lambda^{free}$	0.956	0.522	0.571	0.504
$\Gamma_n/\Gamma_\Lambda^{free}$	0.119	0.273	0.308	0.265

Table 6: Decay rates obtained when considering π, $\pi+K$, $\pi+K$+two-pion and $\pi+K$+two-pion+ω exchange.

Nucleus	$\Gamma_p/\Gamma_\Lambda^{free}$	$\Gamma_n/\Gamma_\Lambda^{free}$	$(\Gamma_p+\Gamma_n)/\Gamma_\Lambda^{free}$	Γ_n/Γ_p	$\Gamma_{tot}/\Gamma_\Lambda^{free}$
${}^{12}_{\Lambda}$C	0.504	0.265	0.769	0.53	1.289
${}^{28}_{\Lambda}$Si	0.665	0.351	1.016	0.53	1.386
${}^{40}_{\Lambda}$Ca	0.694	0.366	1.060	0.53	1.390
${}^{56}_{\Lambda}$Fe	0.754	0.398	1.152	0.53	1.452
${}^{89}_{\Lambda}$Y	0.785	0.414	1.199	0.53	1.499
${}^{139}_{\Lambda}$La	0.765	0.403	1.168	0.53	1.468
${}^{208}_{\Lambda}$Pb	0.847	0.446	1.293	0.53	1.593

Table 7: Decay rates and the Γ_n/Γ_p ratio for different hypernuclei. In Γ_{tot} we have included the contributions from the mesonic decay and the $2p2h$ channel.

has finally a small contribution to the rates because of the cancellation between direct 2π and interference contributions.

It is worth recalling, as we saw from fig. 13, that the σ and uncorrelated 2π contributions have different signs and there are large cancellations between them at the relevant momentum $q \sim 420$ MeV/c. Let us stress once more that we obtain a sign for the σ exchange here which is opposite to the conventional one. Should we have the σ contribution with opposite sign to ours and about the same strength, the combination of σ and uncorrelated two-pion exchange would give a contribution for the 2π part alone about 6 times bigger than here, and this would render the total rates unacceptably large in spite of the interference terms, which are only multiplied by a factor 2.5.

We address now the contribution from the ω exchange. We have already seen in table 6 that the combined effect of the two-pion exchange ("σ" in the table) is very moderate. It increases Γ_p by 10% and Γ_n by 13 %. The inclusion of ω, as looks clear from fig. 15, should give contributions of the same order of magnitude. This is the case indeed, and in table 6 we show the contribution when the ω exchange is added, which indeed is small but helps one to obtain a better agreement with experiment for the total widths.

In table 7 we present the results for Γ_p, Γ_n and the Γ_n/Γ_p ratio for different nuclei. We have used the parameters of ref. [3] for the NNK coupling. We find that the total rates from the $1p1h$ channel go from $\Gamma/\Gamma_\Lambda^{free} = 0.77$ in ${}^{12}_{\Lambda}$C to 1.3 in ${}^{208}_{\Lambda}$Pb and the ratios Γ_n/Γ_p are all of them of about $\Gamma_n/\Gamma_p \sim 0.53$.

We have also made calculations with the couplings for K exchange from [43] and [44]. The qualitative results do not change much. In both cases they lead to smaller ratios and larger widths, particularly in the case of [43], because the strength of the K exchange is smaller and so are the interference terms. However, we should mention that a fit with only three independent terms is done in [43] while there is more freedom, according to [45], where five independent terms contributing to the parity conserving part can be found.

We can also make estimates of possible contributions from heavier mesons like the ρ

Nucleus	$\Gamma/\Gamma_\Lambda^{free}$	Experiment
${}^{9}_{\Lambda}$Be	1.31 ± 0.21[6]	(K^-, π^-)
${}^{11}_{\Lambda}$B	1.37 ± 0.17[6, 47]	(K^-, π^-)
	1.25 ± 0.08[48]	(π^+, K^+)
${}^{12}_{\Lambda}$C	1.25 ± 0.19[6, 47]	(K^-, π^-)
	1.14 ± 0.08[49]	(π^+, K^+)
${}^{16}_{\Lambda}$Z	$3.1^{+1.2}_{-0.9}$[50]	^{16}O beam, K^+ tagging
${}^{27}_{\Lambda}$Al	1.30 ± 0.07[48]	(π^+, K^+)
${}^{28}_{\Lambda}$Si	1.28 ± 0.08[48]	(π^+, K^+)
${}_{\Lambda}$Fe	1.22 ± 0.08[48]	(π^+, K^+)
$\bar{p}+{}^{209}$Bi	$1.1^{+1.1}_{-0.4}$[51]	Delayed fission
	$1.5 \pm 0.3 \pm 0.5$[52]	Delayed fission
$p+{}^{209}$Bi	$1.8 \pm 0.1 \pm 0.3$[53]	Delayed fission
$\bar{p}+{}^{238}$U	$2.6^{+2.2}_{-1.1}$[51]	Delayed fission
	$2.0 \pm 0.5 \pm 0.5$[52]	Delayed fission
$p+{}^{238}$U	1.1 ± 0.3[54]	Delayed fission
	1.4 ± 0.4[55]	re-analysis of [54]
$p+$(Au, U, Bi)	$2.0 \pm 0.2 \pm 0.2$[56]	Delayed fission

Table 8: Experimental values of the total width for different nuclei. The value for ${}_{\Lambda}$Fe represents for the average width of ${}^{55}_{\Lambda}$Mn, ${}^{55}_{\Lambda}$Fe and ${}^{56}_{\Lambda}$Fe.

and the K^*. Given the small range of these exchanges, they can be easily accounted for by means of moderate changes in the g'_Λ parameters of π and K exchange. This is a usual way to account for ρ effects in the effective spin-isospin strong interaction via the Landau-Migdal effective force. We have checked that by increasing the g'_Λ parameter by 20% in the case of the pion or the kaon exchange, the changes in both the Γ_n/Γ_p ratio and the rates were smaller than 5%.

If we want to compare these results with experimental data we should still add the mesonic contribution and the $2p2h$ induced one. For the mesonic contribution we take the results from [46], which agree well with experiment in the measured cases. The mesonic rates are only relevant for the lighter nuclei. We take $\Gamma_M = 0.25\ \Gamma_\Lambda^{free}$ for ${}^{12}_{\Lambda}$C, 0.07 for ${}^{26}_{\Lambda}$Si and 0.03 for ${}^{40}_{\Lambda}$Ca and neglect this contribution for heavier nuclei. The $2p2h$ induced contribution calculated in [23] is $0.27\ \Gamma_\Lambda^{free}$ for ${}^{12}_{\Lambda}$C and 0.30 for the rest of the nuclei. With these results we compute the total rates which we show in table 7. We have recalculated this contribution with the new form factor and with the new values of g' that we use here, rescaling the C_0 parameter of [25] in order to obtain the same strength for the p-wave part of the pionic atoms optical potential. We obtain the same results as in ref. [25], within 5%. The present status of the width measurements can be found in table 8. We can see that our total rates are compatible with the experimental numbers in the best measured nuclei. In heavy nuclei the experimental errors are larger and our results are compatible with the experiment. In fig. 16 we plot our results versus experiment for the total Λ decay width.

As for the Γ_n/Γ_p ratios our results are compatible within the experimental errors, on the lower side. However, one word of caution is necessary here. The experimental analyses were done neglecting the $2p2h$ induced channel, but it was observed in [23] that the inclusion of

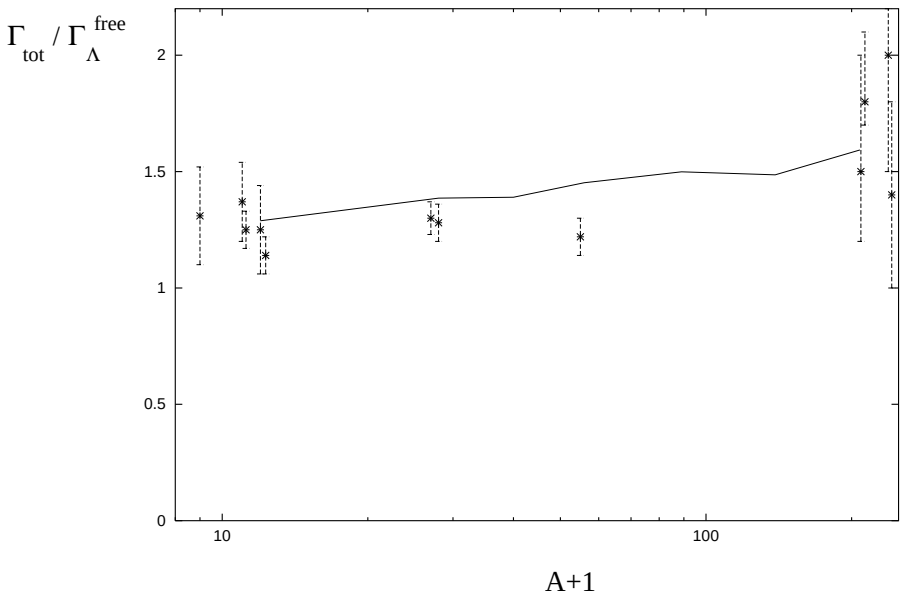

Figure 16: Calculated total Λ decay widths versus experimental data from table 8.

this mechanism in the analyses of the data leads to different values of Γ_n/Γ_p. A formula was given in this reference to correct the results of the old analysis due to the consideration of this induced mechanism, but it assumed that all particles were detected. The formula was corrected in [24] assuming that the slow particles (with energies smaller than about 40 MeV) were not detected. Detailed calculations of the spectra of protons and neutrons from the non-mesonic decay were done in [25] but assuming a ratio of $1p1h$ to $2p2h$ induced strength given by the OPE model alone, which as shown here overcounts the $1p1h$ strength. In view of this we just take the formula of [24] and use it to recalculate the experimental bands. The present bands for ${}^{12}_{\Lambda}$C are: $1.33^{+1.12}_{-0.81}$[6], $1.87^{+0.91}_{-1.59}$ [7], 0.70 ± 0.30[8], 0.52 ± 0.16[8]. The lower bounds are 0.52, 0.29, 0.4, 0.36 respectively. However, if we use the formula of [24] assuming $\Gamma_{2p2h}/\Gamma_{nm}$ of the order of 0.3 one reduces the lower bound to values 0.2, 0.14, 0.1, 0.01 and the value obtained by us is well within present experimental ranges.

6 Conclusions

We have evaluated the non-mesonic proton and neutron induced Λ decay rates in nuclei, by including one pion, one kaon, correlated and uncorrelated two-pion exchange and ω exchange. We found that the contribution of K exchange was essential to reduce the total decay rate from the OPE results and simultaneously increase the value of the Γ_n/Γ_p ratio from values around 0.12 for the OPE to values around 0.52. We also included the σ and uncorrelated two pion exchange and we found some cancellations between them, such that the total contribution of the two-pion exchange to the total rate and the Γ_n/Γ_p ratio was small. Additional inclusion of the ω exchange made the scalar-isoscalar contribution smaller, and while changing the Γ_n/Γ_p ratios only from 0.54 to 0.53, it helped a bit in getting the total rates in better agreement with the data. However, in these results it was very important that the contribution of the σ exchange had opposite sign to the conventional contributions taking only the exchange of a σ particle. This change of sign was due to the

presence of the Adler zero in the scalar-isoscalar $\pi\pi$ interaction which makes the amplitude change sign below $s = \mu^2/2$, which is the case here where we have s negative. We have also evaluated a weak parity violating σ exchange term which we found negligible compared to the parity conserving one.

The total rates obtained are good compared to the present data. The ratios Γ_n/Γ_p are considerably improved with respect to the OPE ones and compatible with present experiments. We have also seen that, once the present experimental data are corrected to account for the $2p2h$ channel the value of 0.53 obtained here for the Γ_n/Γ_p ratio is well within the present experimental boundaries.

Further studies to evaluate the contribution from shorter distances, using for instance quark models, like in [20, 21] would be most welcome. They seem to lead to even larger values of Γ_n/Γ_p but also larger total decay rates. In any case our study of the long and intermediate distances has shown that one can obtain values for Γ_n/Γ_p considerably larger than those given by the OPE model while still having total rates in good agreement with experiment.

Note added in proof

While our paper was in print another related paper appeared in the web [57] paying especial attention to the final state interaction (FSI) of the two nucleons after the Λ decay. Tables IV and V of that paper show the effects of the FSI, but the initial state interaction (ISI) is already accounted for. One should not compare these results with ours, since our correlation function is meant to account for initial as well as final state correlations. Comparison of our results for one pion exchange and ${}^{12}_{\Lambda}$C with those of [57], complemented by the effects of ISI found in [2] is possible. Depending on the strong potential used, the combined effect of ISI and FSI in [57], [2] is a reduction by a factor ranging for 1.4 to 1.9. Our correlation function gives us a reduction of a factor 1.5.

Acknowledgements

We wish to acknowledge multiple and useful discussions with A. Ramos and A. Parreño. Useful information from A. Gal and M. Oka is much appreciated. We would also like to acknowledge financial support from the DGICYT under contracts PB96-0753, PB98-1247 and AEN97-1693, from the Generalitat de Catalunya under grant SGR98-11 and from the EU TMR network Eurodaphne, contract no. ERBFMRX-CT98-0169. J.E.P. thanks finantial support from the Ministerio de Educación y Cultura. The work by D.J. is supported by the Spanish Ministry of Education in the Program "Estancias de Doctores y Tecnólogos Extranjeros en España".

Appendix

In this Appendix we briefly review how to implement the short range correlation in the effective interactions of $\Lambda N \to NN$ and $NN \to NN$. We follow here closely the steps of [58] for this purpose. The hard core in the short range is produced by a strong repulsive force independent on spin and isospin in the NN interaction, and is very well approximated by a local correlation function $g(r)$. Then, we may write the effective interaction G_{NN} through one meson exchange potential $V_{NN\to NN}$ as

$$G_{NN}(r) = g(r)V_{NN}(r) \ , \tag{62}$$

where typically $g(r)$ vanishes as $r \to 0$ and goes to 1 as $r \to \infty$. One of the practical choices of $g(r)$ is

$$g(r) = 1 - j_0(q_c r) \ . \tag{63}$$

The analysis of the NN interaction suggested that eq. (63) with $q_c = 780\text{MeV}/c$ gives a fair correlation function [58].

With eq. (63) the effective interaction in momentum space is given by

$$G_{NN}(q) = [V_l(q)\hat{q}_i\hat{q}_j + V_t(q)(\delta_{ij} - \hat{q}_i\hat{q}_j)]\sigma_i^{(1)}\sigma_j^{(2)}\vec{\tau}^{(1)} \cdot \vec{\tau}^{(2)} \tag{64}$$

with

$$V_l(q) = \frac{f_{\pi NN}^2}{\mu^2}[\vec{q}^{\,2} D_\pi(q) F_\pi^2(q) + g_l(q)] \tag{65}$$

$$V_t(q) = \frac{f_{\pi NN}^2}{\mu^2}[\vec{q}^{\,2} D_\rho(q) F_\rho^2(q) C_\rho + g_t(q)] \tag{66}$$

The short range correlations are taken into account in the $g_l(q)$ and $g_t(q)$:

$$g_l(q) = -\left(\vec{q}^{\,2} + \frac{q_c^2}{3}\right)\tilde{F}_\pi^2(q)\tilde{D}_\pi(q) - \frac{2q_c^2}{3}C_\rho\tilde{F}_\rho^2(q)\tilde{D}_\rho(q) \ , \tag{67}$$

$$g_t(q) = -\frac{q_c^2}{3}\tilde{F}_\pi^2(q)\tilde{D}_\pi(q) - \left(\vec{q}^{\,2} + \frac{2q_c^2}{3}\right)C_\rho\tilde{F}_\rho^2(q)\tilde{D}_\rho(q) \ . \tag{68}$$

The tilde on the functions means that $\vec{q}^{\,2}$ must be changed by $\vec{q}^{\,2} + q_c^2$ in the argument of the function. C_ρ is the ratio of the ρNN coupling to the πNN coupling: $C_\rho = (f_\rho/m_\rho)/(f_{\pi NN}/\mu) = 2$. Here we rescale these functions to keep consistency with the spin-isospin effective nuclear force:

$$g_{l,t}(q) \to g' \frac{g_{l,t}(q)}{g_{l,t}(0)} \tag{69}$$

with $g' = 0.7$. $D_\pi(q)$ and $D_\rho(q)$ are the propagators of π and ρ, respectively, and $F_\pi(q)$ and $F_\rho(q)$ denote the form factor for πNN and ρNN, which are given by

$$F_\pi(q) = \frac{\Lambda_\pi^2}{\Lambda_\pi^2 - q^2} \tag{70}$$

$$F_\rho(q) = \frac{\Lambda_\rho^2 - m_\rho^2}{\Lambda_\rho^2 - q^2} \tag{71}$$

with $\Lambda_\pi = 1.0$ GeV and $\Lambda_\rho = 2.5$ GeV.

Similarly we introduce the short range correlation into the effective interaction $\Lambda N \to NN$:

$$G_{\Lambda N \to NN}(r) = g(r) V_{\Lambda N \to NN}(r) \tag{72}$$

where $V_{\Lambda N \to NN}$ is the potential with one π and K exchanges in this case. We use the same correlation function and q_c for $G_{\Lambda N \to NN}(r)$ and for $G_{NN}(r)$, as usually done.

Then the effective interaction with one π exchange for the parity violating part is written as

$$G_{\Lambda N \to NN}^{\pi,\text{s}-\text{wave}}(q) = V_s'(q)\ \hat{q}_i\ \sigma_i^{(2)}\ \vec{\tau}^{(1)} \cdot \vec{\tau}^{(2)} \tag{73}$$

while the parity conserving part is split into the longitudinal and transverse components:

$$G_{\Lambda N \to NN}^{\pi,\text{p}-\text{wave}}(q) = [V_l'(q)\hat{q}_i\hat{q}_j + V_t'(q)(\delta_{ij} - \hat{q}_i\hat{q}_j)]\sigma_i^{(1)}\sigma_j^{(2)}\vec{\tau}^{(1)} \cdot \vec{\tau}^{(2)} \tag{74}$$

with

$$V_l'(q) = \frac{f_{\pi NN}}{\mu}\frac{P}{\mu}[\vec{q}^2 D_\pi(q) F_\pi^2(q) + g_l^\Lambda(q)] \quad (75)$$

$$V_t'(q) = \frac{f_{\pi NN}}{\mu}\frac{P}{\mu} g_t^\Lambda(q) \quad (76)$$

$$V_s'(q) = \frac{f_{\pi NN}}{\mu} S[D_\pi(q) F_\pi^2(q) + g_s^\Lambda(q)]|\vec{q}| \quad (77)$$

The form factor is assumed to be the same as for the strong πNN vertex. The short range correlations are considered in g_i^Λ:

$$g_l^\Lambda(q) = -\left(\vec{q}^2 + \frac{q_c^2}{3}\right)\tilde{F}_\pi^2(q)\tilde{D}_\pi(q) \quad (78)$$

$$g_t^\Lambda(q) = -\frac{q_c^2}{3}\tilde{F}_\pi^2(q)\tilde{D}_\pi(q) \quad (79)$$

$$g_s^\Lambda(q) = -\tilde{F}_\pi^2(q)\tilde{D}_\pi(q) \quad (80)$$

where the tilde is defined as for the case of the NN interaction.

Similarly, the effective interaction with one kaon exchange are given as

$$G^{K,\mathrm{p-wave}}_{\Lambda N\to NN}(q) = [V_l'^{,K}(q)\hat{q}_i\hat{q}_j + V_t'^{,K}(q)(\delta_{ij} - \hat{q}_i\hat{q}_j)]\sigma_i^{(1)}\sigma_j^{(2)} C_P^{K,N} \quad (81)$$

$$G^{K,\mathrm{s-wave}}_{\Lambda N\to NN}(q) = V_{s,K}'(q)\ \hat{q}_i\ \sigma_i^{(1)}\ C_S^{K,N} \quad (82)$$

with

$$V_{l,K}'(q) = -\frac{f_{K\Lambda N}}{\mu}\frac{P}{\mu}[\vec{q}^2 D_K(q) F_K^2(q) + g_{l,K}^\Lambda(q)] \quad (83)$$

$$V_{t,K}'(q) = -\frac{f_{K\Lambda N}}{\mu}\frac{P}{\mu} g_{t,K}^\Lambda(q) \quad (84)$$

$$V_{s,K}'(q) = -\frac{f_{K\Lambda N}}{\mu} S[D_K(q) F_K^2(q) + g_{s,K}^\Lambda(q)]|\vec{q}| \quad (85)$$

Here $D_K(q)$ is the K propagator and $F_K(q)$ denotes the form factor of the $K\Lambda N$. We use the same form factor for the weak KNN vertex:

$$F_K(q) = \frac{\Lambda_K^2}{\Lambda_K^2 - q^2} \quad (86)$$

with $\Lambda_K = 1.0$ GeV. The short range correlations are accounted for by means of the $g\prime$ coefficients

$$g_{l,K}^\Lambda(q) = -\left(\vec{q}^2 + \frac{q_c^2}{3}\right)\tilde{F}_K^2(q)\tilde{D}_K(q) \quad (87)$$

$$g_{t,K}^\Lambda(q) = -\frac{q_c^2}{3}\tilde{F}_K^2(q)\tilde{D}_K(q) \quad (88)$$

$$g_{s,K}^\Lambda = -\tilde{F}_K^2(q)\tilde{D}_K(q) \quad (89)$$

References

[1] E. Oset, P. Fernandez de Cordoba, L. L. Salcedo and R. Brockmann, Phys. Rept. **188**, 79 (1990).

[2] A. Parreno, A. Ramos and C. Bennhold, Phys. Rev. **C56**, 339 (1997) [nucl-th/9611030] and private communication of recent results.

[3] J. F. Dubach, G. B. Feldman, B. R. Holstein and L. de la Torre, Annals Phys. **249**, 146 (1996) [nucl-th/9606003].

[4] K. Takeuchi, H. Bando and H. Takaki, Prog. Theor. Phys. **73**, 841 (1985).

[5] T. Inoue, S. Takeuchi and M. Oka, Nucl. Phys. **A597**, 563 (1996) [hep-ph/9502392].

[6] J. J. Szymanski *et al.*, Phys. Rev. **C43**, 849 (1991).

[7] H. Noumi *et al.*, Phys. Rev. **C52**, 2936 (1995).

[8] A. Montwill et al., Nucl. Phys. **A234** (1974) 413.

[9] H. Outa *et al.*, Nucl. Phys. **A670**, 281 (2000).

[10] O. Hashimoto, private communication.

[11] E. Oset and A. Ramos, Prog. Part. Nucl. Phys. **41**, 191 (1998) [nucl-th/9807018].

[12] H. Bando, Y. Shono and H. Takaki, Int. J. Mod. Phys. **A3**, 1581 (1988).

[13] M. Shmatikov, Phys. Lett. **B322**, 311 (1994).

[14] K. Itonaga, T. Ueda and T. Motoba, Nucl. Phys. **A585**, 331C (1995).

[15] M. Shmatikov, Nucl. Phys. **A580**, 538 (1994).

[16] C. Y. Cheung, D. Heddle and L. S. Kisslinger, Phys. Rev. **C27**, 335 (1983).

[17] K. Maltman and M. Shmatikov, Phys. Lett. **B331**, 1 (1994).

[18] T. Inoue, M. Oka, T. Motoba and K. Itonaga, Nucl. Phys. **A633**, 312 (1998)

[19] M. Oka, Talk given at the *International Symposium on Nuclear Electro-Weak Spectroscopy (NEWS 99) for Symmetries and Electro-Weak Nuclear-Processes*, Osaka, Japan, 9-12 Mar 1999 nucl-th/9906041.

[20] K. Sasaki, T. Inoue and M. Oka, Nucl. Phys. **A669** (2000) 331 [nucl-th/9906036] ; erratum **A**678, 455 (2000).

[21] M. Oka, talk given at Hyper2000 conference, Torino, October 2000.

[22] W. M. Alberico, A. De Pace, M. Ericson and A. Molinari, Phys. Lett. **B256**, 134 (1991).

[23] A. Ramos, E. Oset and L. L. Salcedo, Phys. Rev. C **50**, 2314 (1994).

[24] A. Gal, In *Osaka 1995, Weak and electromagnetic interactions in nuclei* 573-574.

[25] A. Ramos, M. J. Vicente-Vacas and E. Oset, Phys. Rev. **C55**, 735 (1997)

[26] E. Oset, H. Toki, M. Mizobe and T. T. Takahashi, Prog. Theor. Phys. **103**, 351 (2000) [nucl-th/0011008].

[27] J. Gasser and H. Leutwyler, Ann. Phys. NY **158** (1984) 142; J. Gasser and H. Leutwyler, Nucl. Phys. **B250** (1985) 465, 517, 539; A. Pich, Rep. Prog. Phys. 58 (1995) 563; G. Ecker, Prog. Part. Nucl. Phys. 35 (1995) 1; U.-G. Meißner, Rep. Prog. Phys. 56 (1993) 903.

[28] J. A. Oller and E. Oset, Nucl. Phys. **A620**, 438 (1997) [hep-ph/9702314]; Erratum, A652 (1999) 407.

[29] A. Parreno and A. Ramos, private communication.

[30] E. Oset and L. L. Salcedo, Nucl. Phys. **A443**, 704 (1985).

[31] E. Oset, M. Rho, Phys. Rev. Lett. **42** (1979), 42; H.C. Chiang, E. Oset, P. Fernandez de Cordoba Nucl. Phys. **A510** (1990), 591.

[32] A. Parreno, C. Bennhold, A. Ramos, to be published, private communication.

[33] K. Itonaga, T. Ueda and T. Motoba, Nucl. Phys. **A639**, 329 (1998).

[34] A. Dobado and J. R. Pelaez, Phys. Rev. D **56**, 3057 (1997) [hep-ph/9604416].

[35] J. A. Oller, E. Oset and J. R. Pelaez, Phys. Rev. Lett. **80**, 3452 (1998) [hep-ph/9803242].

[36] J. A. Oller and E. Oset, Phys. Rev. D **60**, 074023 (1999) [hep-ph/9809337].

[37] V. E. Markushin, Eur. Phys. J. **A8**, 389 (2000) [hep-ph/0005164].

[38] J. C. Nacher, A. Parreno, E. Oset, A. Ramos, A. Hosaka and M. Oka, Nucl. Phys. **A678**, 187 (2000) [nucl-th/9906018].

[39] E. Oset and A. Ramos, Nucl. Phys. **A679**, 616 (2001) [nucl-th/0005046].

[40] A. Jackson, A. D. Jackson and V. Pasquier, Nucl. Phys. A **432** (1985) 567.

[41] R. B. Wiringa, R. A. Smith and T. L. Ainsworth, Phys. Rev. C **29** (1984) 1207; R. B. Wiringa, V. G. Stoks and R. Schiavilla, Phys. Rev. C **51** (1995) 38 [nucl-th/9408016].

[42] M. R. Robilotta and C. A. da Rocha, Nucl. Phys. A **615** (1997) 391 [nucl-th/9611056].

[43] J. Schaffner-Bielich, R. Mattiello and H. Sorge, Phys. Rev. Lett. **84**, 4305 (2000) [nucl-th/9908043].

[44] M. J. Savage and R. P. Springer, Phys. Rev. C **53**, 441 (1996) [hep-ph/9508287].

[45] R. E. Marshak, Riazuddin, C. P. Ryan, *Theory of weak interactions in particle physics*, edited by Wiley-Interscience, 1969.

[46] J. Nieves and E. Oset, Phys. Rev. C **47**, 1478 (1993).

[47] R. Grace *et al.*, Phys. Rev. Lett. **55**, 1055 (1985).

[48] H. Park *et al.*, Phys. Rev. C **61**, 054004 (2000).

[49] H. Bhang *et al.*, Phys. Rev. Lett. **81**, 4321 (1998).

[50] K. J. Nield *et al.*, Phys. Rev. C **13**, 1263 (1976).

[51] J. P. Bocquet *et al.*, Phys. Lett. **B192**, 312 (1987).

[52] T. A. Armstrong *et al.*, Phys. Rev. **C47**, 1957 (1993).

[53] P. Kulessa *et al.*, Phys. Lett. **B427**, 403 (1998).

[54] H. Ohm *et al.*, Phys. Rev. **C55**, 3062 (1997).

[55] I. Zychor, et al., *Int. Symp. on Nuclear Electro-Weak Spectroscopy for Symmetries and Electro-Weak Nuclear processes* (NEWS99), Osaka University, Osaka, Japan.

[56] B. Kamys, P. Kulessa, H. Ohm, K. Pysz, Z. Rudy, H. Stroher and W. Cassing, hep-ex/0011063.

[57] A. Parreño and A. Ramos, nucl-th/0104080

[58] E. Oset and W. Weise, Nucl. Phys. **A319**, 477 (1979).